#### **RESEARCH PAPER**



# Experimental investigation of mechanical and microstructural properties of re-cemented clay

Wei-Feng Huang<sup>1</sup> · Zhi-Jian Ruan<sup>1</sup> · Ding-Bao Song<sup>1,2</sup> · Dian-Long Wang<sup>1</sup> · Ma-Yao Cheng<sup>3</sup>

Received: 24 November 2024 / Accepted: 1 April 2025 / Published online: 26 June 2025 © The Author(s) 2025

#### **Abstract**

Considerable amounts of cemented mixtures are generated during the construction of deep cement mixing piles. Recycling these generated cemented soils as fill material using re-cemented method can reduce waste transfer to landfills and reduce the use of natural gravel fill resources. However, the properties of these re-cemented materials remain unclear. To fill this research gap, in this study, cement-treated Hong Kong marine deposit (CT-HKMD) was ground into powders and used as a reused material for the second-round cement treatment, named recycled cement-treated Hong Kong marine deposit (RCT-HKMD). The influences of cement content and curing period on the unconfined compressive and tensile strengths, modulus, point load strength index and phase assemblage of CT-HKMD and RCT-HKMD were investigated through unconfined compression (UC) tests, Brazilian tests, point load tests and thermogravimetric analysis (TGA). The results reveal that the unconfined compressive strength (UCS), splitting tensile strength and point load strength index of RCT-HKMD are 1.3–2.6 times greater than those of CT-HKMD within the same cement content and curing period. This is due to denser microstructure and the formation of calcium (alumino) silicate hydrate (C-(A-)S-H) and ettringite to fill into the small pores and improve interparticle bonding, observed from the results of TGA and scanning electron microscopyenergy-dispersive spectrometer (SEM-EDS). Furthermore, different initial cement contents of CT-HKMD powders were used to prepare RCT-HKMD specimens with 10% newly cement content. All test results show that the initial cement content of CT-HKMD has no effect on the UCS, splitting tensile strength and point load strength index of RCT-HKMD specimens as the original bonding structures of the CT-HKMD have been destroyed after crushing and sieving process. All the findings have practical implications for the reuse of waste cemented soil locally and even globally.

**Keywords** Brazilian tests · Cements · Point load tests · Scanning electron microscope · Thermogravimetric analysis · Unconfined compression tests

- ☑ Ding-Bao Song dingbao.song@polyu.edu.hk; dingbao\_song@126.com
  - Wei-Feng Huang 24151775r@connect.polyu.hk

Zhi-Jian Ruan james.ruan@connect.polyu.hk

Dian-Long Wang dianlong.wang@polyu.edu.hk

Ma-Yao Cheng chengmayao@163.com

Department of Civil and Environmental Engineering, The Hong Kong Polytechnic University, Hong Kong, China

- Research Centre for Resources Engineering Towards Carbon Neutrality (RCRE), The Hong Kong Polytechnic University, Hong Kong, China
- School of Civil Engineering and Transportation, Foshan University, Foshan, China



#### 1 Introduction

Due to the scarcity of backfill material, the limited capacity of landfills and other environmental concerns, recycling waste materials such as marine clay and cemented soil is becoming increasingly important. The continuous growth of the global construction industry has led to the consumption of large quantities of natural aggregates, backfill materials such as gravel and sand, which are widespread in nature [23, 40]. As the needs of the global population continue to increase, more and more land is being expropriated for residential, infrastructure and other uses, which not only leads to less available land area, but also makes it difficult to build a new landfill, especially in Hong Kong. In recent years, dredged soil, as one of the wastes, has been extensively studied for beneficial reuse as fill material [52, 54]. Additionally, various types of waste such as excavated muck, construction waste and cemented soil for the construction of embankments, subgrades and artificial islands have also been studied [11, 56, 58].

Cemented soil, a by-product of deep cement mixing (DCM), is frequently generated during this foundation improvement technique, which has been widely used in recent decades to treat problematic or soft soils [18, 26, 27]. A significant environmental challenge of DCM technique is the production of substantial amounts of solid waste such as cemented soil. At the conclusion of DCM process, the drill pipe is extracted, bringing a large amount of cemented mixture to the surface as waste cemented soil. It is estimated that waste cemented soil constitutes about 30% of the total volume involved in the DCM process [16]. Additionally, in reclamation projects such as D-runway of the Tokyo International Airport [59], cement is added to rapidly improve the soft soil, but much of this cemented soil is subsequently removed during the excavation process for foundation or basement construction. In many countries, this waste is typically disposed of in landfills, leading to low recycling rates, diminished landfill capacity and high transportation costs [38, 47]. Therefore, investigating more efficient methods to manage waste cemented soil is crucial such as recycling as backfill material used in reclamation projects.

The properties of cemented soil are complex and affected by the soil particle size, cement content, curing time, water content, etc. [14, 42, 45, 53]. Numerous studies have shown that the mechanical properties of cemented soil improve with increasing cement content and curing period, resulting in the formation of more structured cemented soil [13, 17, 31, 36]. However, there are very few studies on the re-cemented soil, and there is no clear and unified conclusion on the relationship between point load strength index and UCS, point load strength index and tensile

strength and UCS and tensile strength. These parameters are important in both research and practical engineering to better understand mechanical properties of cemented and re-cemented soil for designing safety foundations, slopes or embankments within cement stabilization. Recent studies indicated that powdered reused materials can be utilized in cemented soil to improve the strength properties of cemented soil [5, 46]. Nakayenga et al. [46] demonstrated that incorporating stone powder into cemented soil can increase shear strength and unconfined compressive strength (UCS) with the smallest particle size of stone powder exhibiting the highest UCS. Baldovino et al. [5] illustrated that glass powder can be utilized in cemented soil to improve UCS with the greater glass powder content yielding the higher UCS. As a result, Watabe et al. [58] used the same method that was ground the cemented soil into powder (smaller than 0.425 mm) and reused the powder in re-cemented soil and proved that when the cement content and curing period were the same, there was no significant difference in the UCS and microstructure of the cemented soil and re-cemented soil. Nevertheless, the evolution of tensile strength, point load strength index, modulus and microstructure of re-cemented soil is still lacking. It is also important to point out that no UCSmodulus, UCS-tensile strength, UCS-point load strength index, tensile strength-modulus, point load strength indextensile strength and point load strength index-modulus relationships of re-cemented soil have been established, so further research is required.

This paper reports on an experimental study that aims to investigate the mechanical and microstructure properties of re-cemented soil considering the effect of cement content and curing period when the original cemented soil is remodeled and used as a reused material for the secondround cement treatment. The results of the study reveal the effects of the water/cement ratio, w/c, and the curing period on the mechanical and microstructural properties of the cemented soil and re-cemented soil and also show the influence of cemented history on the performance of the recemented soil to prove the potential use of recycled cemented soil as a backfill material and promote sustainable development. In addition, the relationship between unconfined compression test result and Brazilian test result, unconfined compression test result and point load test result and Brazilian test result and point load test result have been studied to help engineers easily design cemented soil strength and analyze settlement.



Table 1 Geotechnical properties of HKMD

Liquid limit (%)	Plastic limit (%)	Plastic index (%)	Specific gravity (g/ cm <sup>3</sup> )	pH value	Loss of ignition (%)	
49.7	25.8	23.9	2.63	9.06	4.66	

#### 2 Materials and methods

# 2.1 Hong Kong marine deposits and cemented soil powder

HKMD, the soil used in this study, was taken from a construction site located in Tung Chong, Hong Kong. The geotechnical properties of these soils including liquid limit, plastic limit, specific gravity and pH value were tested and the results are listed in Table 1. According to British Standards [8], this soil is classified as intermediate plasticity clay (CI). From the particle size distribution (PSD) results, HKMD is found to be composed of 16.5% fine gravel, 20.6% sand, 50.1% silt and 12.8% clay size fraction. The SEM image of HKMD which is displayed in Fig. 2 shows HKMD has an open type of microstructure with massive clay particles assembled in a dispersed arrangement. The chemical composition of HKMD was investigated through X-ray fluorescence (XRF) that mainly consists of SiO<sub>2</sub>, Al<sub>2</sub>O<sub>3</sub> and Fe<sub>2</sub>O<sub>3</sub>. These compounds are commonly found in marine clay and play an active role in the cement stabilization process such as hydration process. Besides, the organic matter content of HKMD was determined by the loss-on-ignition method that was 4.66%. This organic matter content is very low and has a negligible impact on the hydration reaction of cement. As Ge et al. [20] demonstrated that when the content of humic acid, one of the main organic matters in soil, exceeded 15%, the UCS of cemented soil would be greatly decreased, with reductions exceeding 12%.

As Kitazume [33] recommended, the maximum grain size of the sieved sample should be less than one-fifth of the inner diameter of the mold that should be 10 mm in this study, and there were still lots of stones and shells in the HKMD resulting in inaccurate test results. Hence, the collected HKMD was sieved by 5 mm firstly to remove great number of stones and shell pieces and dried in an oven at 105 °C of temperature to constant mass secondly and finally added distilled water up to 60% water content that closed to the water content of in situ HKMD in Hong Kong.

Cemented soil powder, frequently used in this report to prepare re-cemented soil, is obtained from cemented soil with 10% cement content and 28-day curing. To enhance

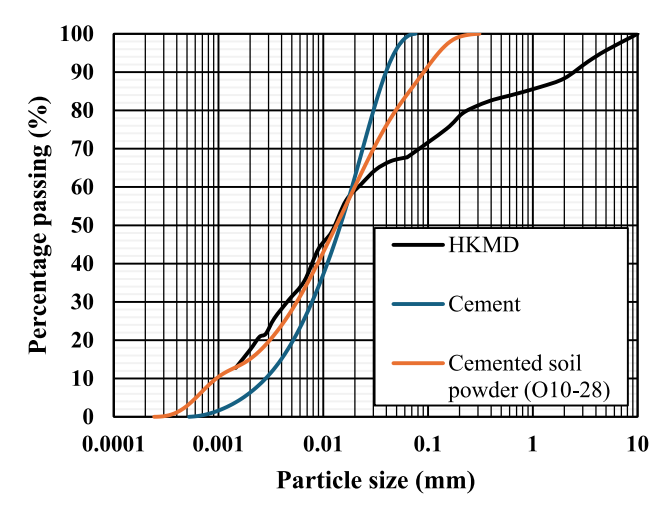


Fig. 1 Particle size distribution of HKMD, cement and cemented soil powder (O10-28)

the accuracy of test results for re-cemented soil, as reported by Watabe et al. [58], the cemented soil was sieved to 0.425 mm into powder for preparing re-cemented soil. This can minimize the presence of coarse particles and improve the uniformity of the re-cemented soil specimen. The details will be introduced in the unconfined compressive strength results. The particle size distribution, SEM image and chemical composition of this powder are shown in Figs. 1 and 2 and Table 2.

#### 2.2 Binder materials

Ordinary Portland cement (OPC) 42.5, which is used frequently as one of the binder materials in Hong Kong, was used in this study. The OPC 42.5 was sourced from Green Island Cement Company Limited in Hong Kong to ensure compositional consistency.

#### 2.3 Specimen preparation

To prepare CT-HKMD specimen, the HKMD with 60% water content was mixed firstly to obtain homogenous HKMD slurry and then added cement slurry. The cement slurry has a *w/c* ratio of 1 that was commonly used [6], and the cement contents used were 5%, 10%, 15% and 20% by dry mass of soil. All the materials were mixed using an electric mixer for 10 min to form a uniform mixture and then poured into cylindrical plastic molds (50 mm in diameter and 100 mm in height). The mold was coated with oil to the inner surface to reduce the friction between the specimen and inner surface for easy demolding. During specimen preparation, the fresh mixture was poured up to one-third of the height of cylindrical plastic mold each time and shaken using a vibration table for 1 min each time to remove inside air voids. After that, to ensure the



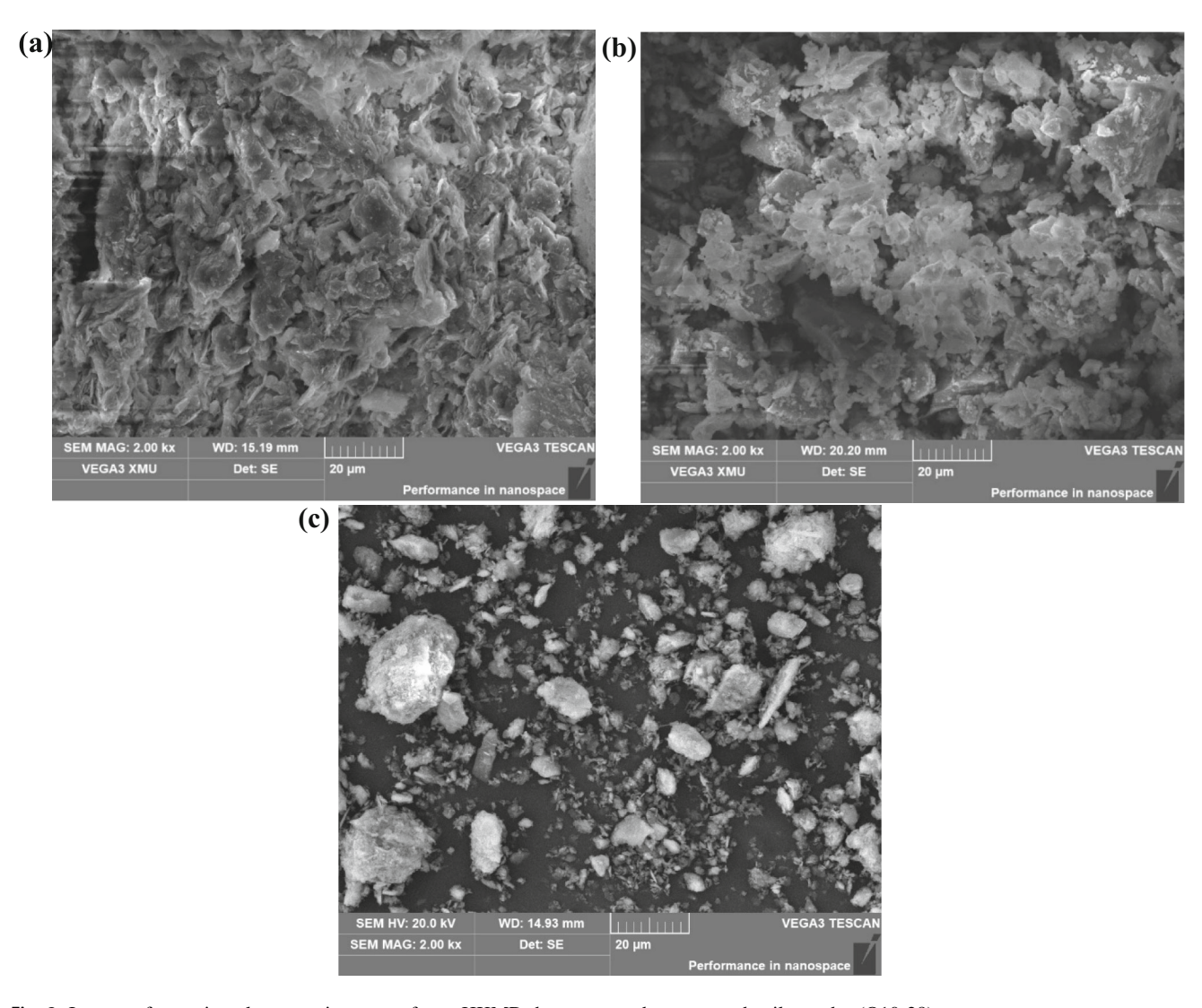


Fig. 2 Images of scanning electron microscope for: a HKMD, b cement and c cemented soil powder (O10-28)

Table 2 Major chemical compositions of HKMD, OPC 42.5 and cemented soil powder (wt. %)

	MgO	$Al_2O_3$	SiO <sub>2</sub>	$SO_3$	Cl	$K_2O$	CaO	TiO <sub>2</sub>	MnO	$Fe_2O_3$	CuO	ZnO	Rb <sub>2</sub> O	SrO	ZrO <sub>2</sub>
HKMD	5.03	18.8	53.2	2.57	1.03	4.2	4.28	1.33	0.13	9.26	0.02	0.02	0.03	0.04	0.04
OPC 42.5	1.01	4.19	14.6	3.68	_	_	70	_	-	4.78	_	-	-	_	-
Cemented soil powder (O10-28)	4.09	15.3	44.7	2.57	0.89	3.59	15.2	1.21	0.12	8.86	0.04	0.04	0.03	0.05	0.02

smoothness of specimen surfaces, the mixture was trimmed using a palette knife and then was covered by plastic films and sealed with electrical tape to avoid changes in water content caused by evaporation. All the sealed molds were cured at 21 °C  $\pm$  1 °C and with relative humidity around 95%. After 7 days, the specimens gained sufficient strength and were demolded and re-sealed to minimize exchange of the water content and cured in the same condition as

previously until the target curing period. The proposed mixing specimen is shown in Table 3 with a total of 6 group mixtures that examine the effects of cement contents with 5%, 10%, 15% and 20% and curing periods with 7, 14 and 28 days based on 10% cement content, and each mixture includes seven parallel specimens for conducting UC test, Brazilian test, point load test, SEM and TG analysis.



Table 3 Proposed mixing specimens

Type	Specimen ID	Cement content (%)	Curing period (day)	Note	Test		
CT- HKMD	O5-28	5	28	First round cementation (effect of cement	UC test Brazilian test and point load test		
	O10-7	10	7	content and curing period)			
	O10-14	10	14				
	O10-28	10	28				
	O15-28	15	28				
	O20-28	20	27				
RCT- HKMD	O10-14- R10-14	R10-14 10-28-	14	Second-round cementation (effect of 5-mm and 0.425-mm sieve for preparing re-cemented soil)	UC test Brazilian test and point load test		
	O10-28- R10-14						
RCT- HKMD	O5-28- R5-28	5	28	Second-round cementation (difference of mechanical and microstructural properties between cemented	UC test Brazilian test and point load test		
	O10-28- R10-28	10		soil and re-cemented soil with the same cement content and curing period)			
	O15-28- R15-28	15					
	O20-28- R20-28	20					
RCT- HKMD	O10-28- R10-28	10	28	Second-round cementation (effect of cemented history)	UC test Brazilian test and point load test		
	O15-28- R10-28						
	O20-28- R10-28						
RCT- HKMD	O10-28- R5-7	5	7	Second-round cementation (effect of cement content and curing period)	UC test Brazilian test and point load test		
	O10-28- R5-14	5	14				
	O10-28- R5-28	5	28				
	O10-28- R10-7	10	7				
	O10-28- R10-14	10	14				
	O10-28- R10-28	10	28				
	O10-28- R20-7	20	7				
	O10-28- R20-14	20	14				
	O10-28- R20-28	20	28				

'O10-28' presents to original cemented soil with 10% cement content and 28-day curing; 'O10-28-R20-28' refers to re-cemented soil with 20% cement content and 28-day curing that the raw material is prepared from original cemented soil with 10% cement content and 28-day curing



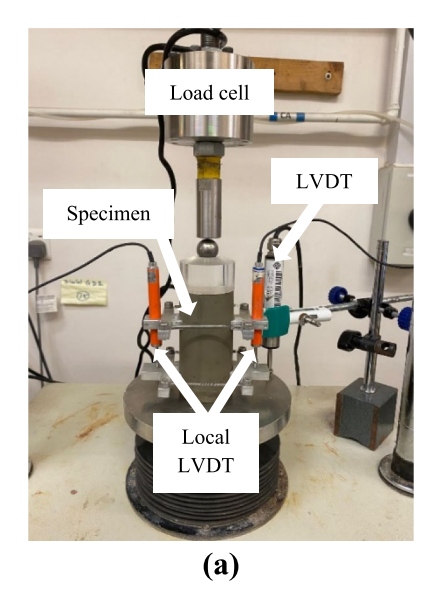
Test soil for RCT-HKMD was prepared by CT-HKMD powder. CT-HKMD specimens with 5%, 10%, 15% and 20% cement contents and 28-day curing were firstly dried in an oven at 105 °C of temperature to constant mass, which was consistent with the situation at the site, that was, the waste cemented soil would be stacked nearby to be exposed to the sunlight firstly [38]. Subsequently, these specimens would be crushed and sieved by 0.425-mm mesh to destroy the structure of CT-HKMD specimens and reduce large particles and finally these CT-HKMD powders were placed back in the oven to ensure adequate dryness. To prepare RCT-HKMD specimen, CT-HKMD powders were mixed with a certain amount of distilled water that water content was 60% and then add cement slurry that has the same w/c ratio mentioned above. The following specimen preparations are the same as above. The proposed mixing specimens are also listed in Table 3 with a total of 16 group mixtures which study the effect of cement contents, curing periods and cemented history and each mixture also has seven parallel specimens.

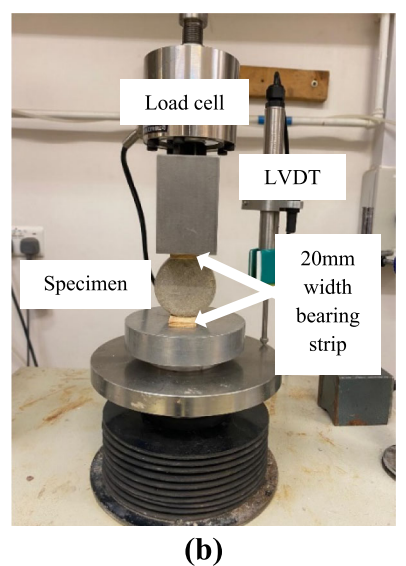
#### 2.4 Testing methods

The UC test of the specimens was performed according to ASTM D2166 [3]. For each mixture, three specimens were tested to ensure consistency of the results obtained and the average results of triplicate specimens were used to determine the UCS. The test was conducted using a VJ-Tech Tri-Scan 50 triaxial test machine, as shown in Fig. 3, and a constant loading rate of 0.5 mm/min that is the lowest loading rate in ASTM D2166 [3] to collect more small strain data. The axial loading of the specimens was

measured using a load cell. The global vertical strain of the specimens was measured using a 50-mm linear variable differentiate transformer (LVDT), and the local vertical strain of the specimens was measured using two 5-mm LVDTs to estimate the effects of seating or bedding error.

The Brazilian test of the specimens was performed according to ASTM C496 [4]. For each mixture, three specimens were tested, and the average results of triplicate specimens were used to determine the tensile strength. As shown in Fig. 3, the VJ-Tech Tri-Scan 50 triaxial test machine was used at a constant loading speed of 0.25 mm/ min to perform the Brazilian test since the tensile strength with 0.5-0.005 mm/min was almost the same [30], and a faster rate was adopted in this study. The axial loading of the specimens was measured using a load cell. The global vertical strain of the specimens was measured using a 50-mm LVDT. Before testing, the top and bottom surface of specimens with 50 mm in diameter and 100 mm in height will be cut by automatic cutting machine and then cut three small specimens with 25 mm in height and 50 mm diameter for the Brazilian test. Additionally, there are different types of Brazilian test setup, for example: Flat loading platens with wooden strips (Type I), flat loading platens with two small diameter steel rods (Type II) and curved loading jaw (Type III). For the case of Type II, the severe stress concentrations existing in the vicinity of the loading points create a wedge-shaped crushed region, causing the crack initiation point to be located at the end of the specimen [60]. This contradicts the assumptions of the Brazilian test that the crack initiation point should be closed to the center of the specimen, leading to an invalid splitting tensile strength. In the case of Type III,





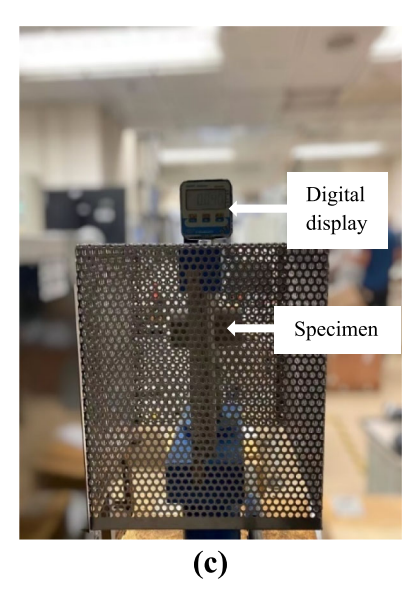


Fig. 3 Photographs of testing setups for: a unconfined compression test, b Brazilian test, and c point load test



catastrophic crushing failure occurs instead of tensile splitting due to shear stress generated under the loading platen, compromising the accuracy of splitting tensile strength [34]. Conversely, Type I avoids the issues associated with Type II and III. It primarily experiences tensile splitting with the crack initiation point located at the center of the specimen, meeting the assumptions of the Brazilian test and ensuing accurate splitting tensile strength [60]. Thus, Type I is used for the Brazilian test in this study.

To understand the relationship between the point load strength index and various parameters including UCS, tensile strength and modulus of cemented and re-cemented soil, the point load test of the specimens was conducted according to ASTM D5731 [2] that is shown in Fig. 3. The maximum point load of the specimens was recorded by the digital display. For each mixture, three specimens were tested, and the average results of those specimens were used to determine the point load strength.

Each mixture has a parallel specimen, and after the target curing period arrived, the parallel specimen was frozen-dried in a freeze-drier (Labconco Freezone 2.5 Plus) for 48 h. Then, some of the frozen specimens were crushed into fine powders to achieve homogeneity for TG analysis and the block park of the frozen specimens was used for SEM-EDS test. For TG analysis (Rigaku STA8122), around 10 mg frozen-dried powder of each mixture was heated at a rate of 10 °C/min until 950 °C. Argon gas was made to flow at a rate of 0.1 L/min during the TG analysis to prevent carbonation. The morphology and microstructure of each mixture were analyzed by SEM-EDS on TESCAN VEGA 3 in the secondary electron mode.

## 3 Results and discussion

#### 3.1 Unconfined compression strength

Figure 4 presents the preliminary tests results to find whether the 5-mm (O10-14-R10-14) or 0.425-mm (O10-28-R10-14) sieve is suitable for preparing the re-cemented soil. The stress-strain curve for O10-14-R10-14 clearly shows a significant turning point that affects the results of peak stress, failure strain and secant Young's modulus, and this is attributed to the unevenness of the specimen. After being crushed and sieved with a 5-mm sieve, the cemented soil still contained lots of coarse particles and the fluidity was also poor after mixing with cement slurry, leading to low specimens' uniformity. Consequently, the coarse particles were continuously crushed into fine particles during the test. To reduce the impact of unevenness in the recemented soil and obtain accurate peak stress, failure strain and secant Young's modulus results, a 0.425-mm sieve is

used for preparing re-cemented soil, as referenced in Watabe [58].

The typical stress–strain curves of the two specimens named O5-28 and O5-28-R5-28 are shown in Fig. 5. It is observed that both global strains are significantly larger than local strain which can be possibly due to sitting error, bedding error or compliance error when axial strain was measured by global LVDT [25, 55]. The typical stress–strain curves also investigate that CT-HKMD and RCT-HKMD specimens display strain softening behavior because of cementation [28]. In addition, the axial strain at failure ( $\varepsilon_f$ ) of CT-HKMD and RCT-HKMD specimens is plotted against the UCS on Fig. 6. The axial strains at failure range from 1.3 to 2.4% for CT-HKMD specimens while 1.6–3.4% for RCT-HKMD specimens. The  $\varepsilon_f$  appears to decrease with increasing UCS that is consistent with other research on cement-treated soil [39].

UCS, secant Young's modulus ( $E_{\text{sec.}50}$ ) and small strain elastic modulus  $(E_0)$  can be determined from the stressstrain curve, and both are of great significance for evaluating the bearing capacity and settlement analysis of foundation when cemented soil is utilized as the bearing stratum. Figures 7 and 8 illustrate the influence of the water/cement ratio on the UCS,  $E_{\text{sec},50}$  and  $E_0$  for both types of soils. It is evident that the cement content significantly influences the UCS of both cemented soils. Even a small addition of cement can lead to a substantial improvement in UCS. Besides, regardless of whether the specimen is CT-HKMD or RCT-HKMD, the UCS,  $E_{\text{sec},50}$ and  $E_0$  increase with decreasing water/cement ratio, which attributed to more complete stabilization reactions in the mixture such as hydration reaction [36, 58]. As the water/ cement ratio reduces, the hydration reaction will be more significant, leading to more calcium ions being dissolved

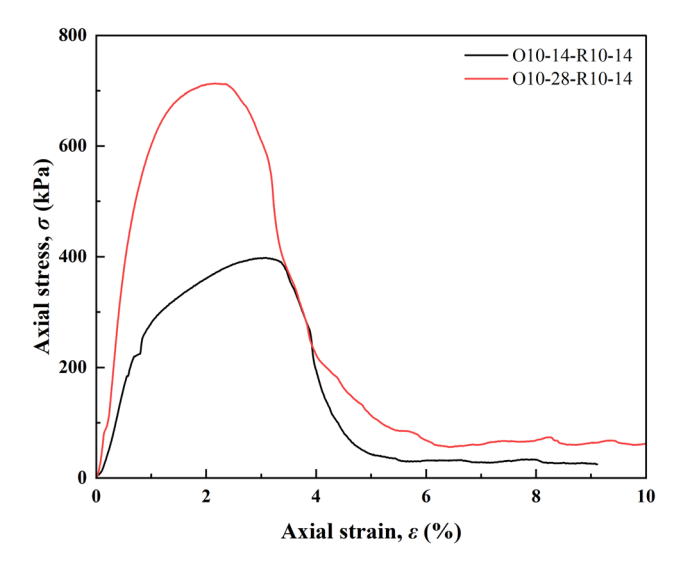
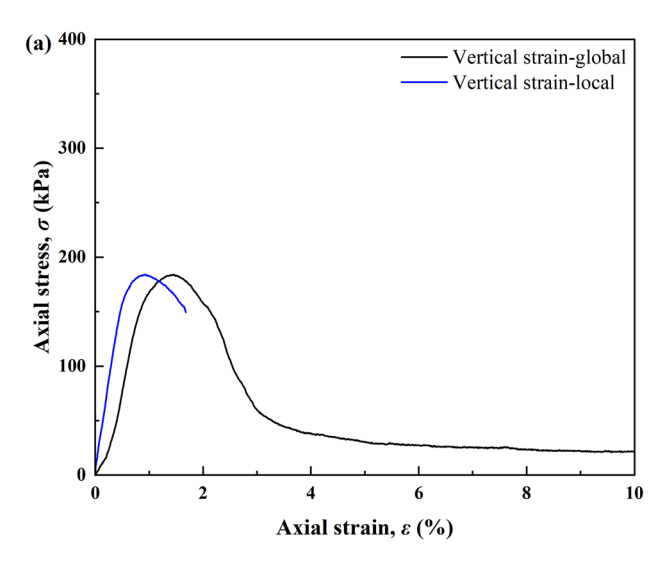


Fig. 4 Stress-strain curve of O10-14-R10-14 and O10-28-R10-14





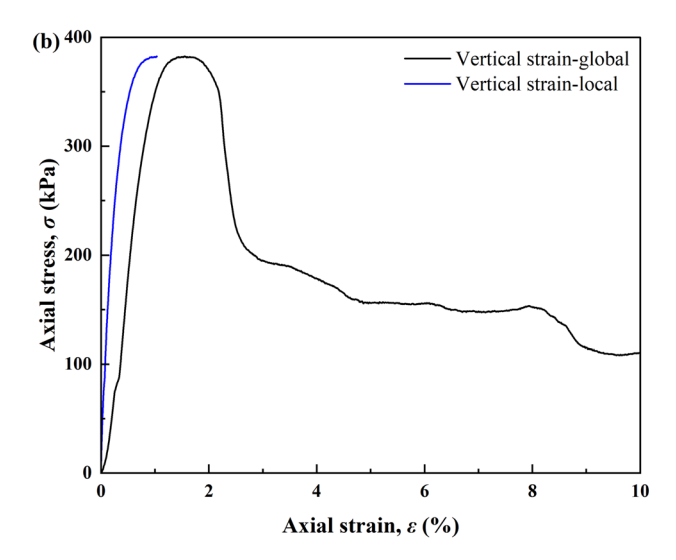


Fig. 5 A typical stress-strain curve of UC test of specimens: a CT-HKMD and b RCT-HKMD

and more hydration products being formed, such as ettringite (AFt) [15]. These hydration products can bind soil particles together to form a new soil matrix that is more cohesive.

Another feature that can be seen in Figs. 7 and 8 is the UCS,  $E_{\text{sec},50}$  and  $E_0$  exhibit a strong power relationship, as shown below, with water/cement ratio with high correlation coefficient. This demonstrates that water/cement ratio has a strong dominant effect on UCS,  $E_{sec,50}$  and  $E_0$  and can be used to simply predict above parameters over various cement content and raw materials in cemented soil. Also, similar patterns of improvement shown in Fig. 7 were observed in cement-treated Bangkok clay [29] and cement-treated Singapore marine clay [36] indicated that the findings in this study were not limited to nature HKMD. However, it is worth to mention that the experimental data presented in Fig. 8 show an unstable trend, that is, the changes of a and b for cemented soil irregularly with curing period. As a result, these fitting equations can only be used for a specific curing period.

$$q_u \text{ or } E_{\text{sec},50} \text{ or } E_0 = a \left(\frac{w}{c}\right)^b$$
 (1)

where  $q_u$  represents the UCS,  $E_{\text{sec},50}$  is the secant Young's modulus,  $E_0$  means the small strain elastic modulus, and a and b refer to experimentally fitted coefficients.

Since it is unclear whether there are differences in the mechanical properties between cemented and re-cemented soil at the same cement content and curing period, the UCS and modulus of both types of soils with the same cement content and curing period were studied. Comparing the UCS,  $E_{\rm sec.}$ , 50 and  $E_0$  of CT-HKMD specimens and RCT-

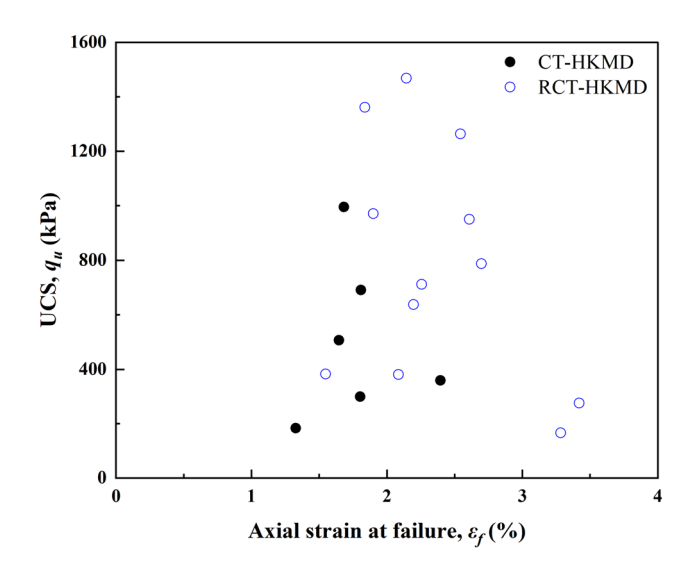


Fig. 6 Axial strain at failure versus UCS

HKMD specimens with the same cement content and curing period, the  $\alpha$ ,  $\beta$  and  $\eta$  are calculated as follows:

$$\alpha = \frac{q_u^R}{q_u^C} \times 100\% \tag{2}$$

$$\beta = \frac{E_{\text{sec},50}^R}{E_{\text{sec},50}^C} \times 100\% \tag{3}$$

$$\eta = \frac{E_0^R}{E_0^C} \times 100\% \tag{4}$$

where  $q_u^R$  and  $q_u^C$  are the UCS of RCT-HKMD and CT-HKMD specimens,  $E_{\sec,50}^R$  and  $E_{\sec,50}^C$  refer to the secant Young's modulus of RCT-HKMD and CT-HKMD



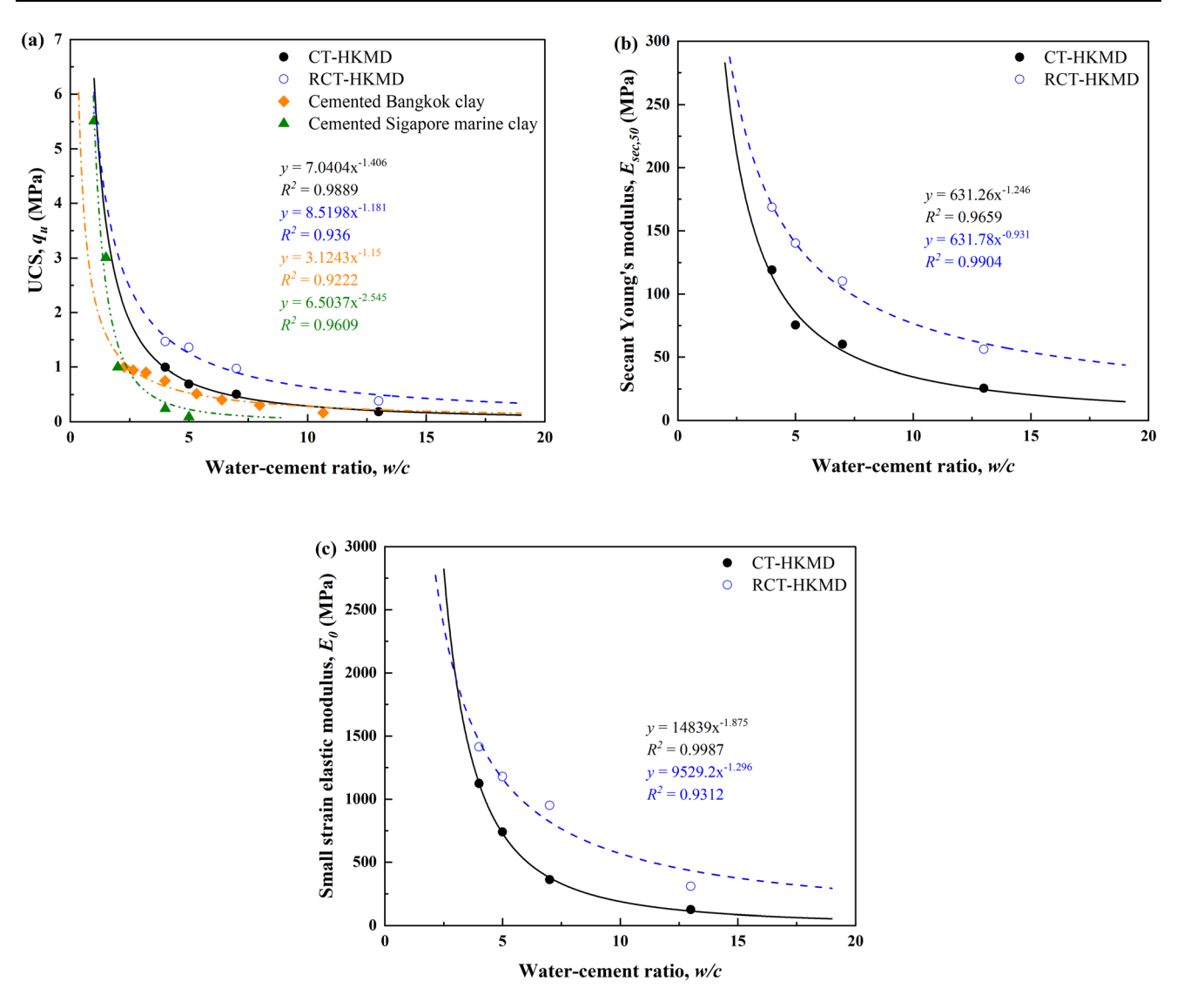


Fig. 7 UC test results (based on w/c ratio with same cement content and curing period between cemented and re-cemented soil): a UCS, b  $E_{sec,50}$  and c  $E_0$ 

specimens, and  $E_0^R$  and  $E_0^C$  represent the small strain elastic modulus of RCT-HKMD and CT-HKMD specimens, respectively.

In detail, the UCS,  $E_{\rm sec,50}$  and  $E_0$  of RCT-HKMD specimens experienced an improvement of around 130% to 260% compared to CT-HKMD specimens with the same cement content and curing period that is shown in Fig. 9. This indicates that cemented soil powder, as a waste material, but used in this study as a raw material for recemented soil, is more effective in improving the UCS,  $E_{\rm sec,50}$  and  $E_0$  relative to that of cemented soil. The improvement of the UCS,  $E_{\rm sec,50}$  and  $E_0$  in RCT-HKMD specimens can be caused by the denser microstructure. The CT-HKMD powders below 0.425 mm were used for preparation of RCT-HKMD specimens with small pores and more contact points between soil particles [45]. During

stabilization reaction, hydration products such as calcium silicate hydrate (C-S-H) only need to fill small pores and soil particles are easily connected with more hydration products precipitated between the particle contacts, resulting in the denser microstructures of specimens that will discuss in results of SEM. Besides, the crushing process for the cemented soil to prepare re-cemented soil can change the particle size distribution and structure of the cemented soil, which affects the density and contact points between soil particles or clusters and cement powder [50]. At the same time, the finer mesh used in the sieving process to prepare re-cemented soil can increase the fine content with smaller voids, leading to greater density and strength of re-cemented soil.

To quantify the relationship between the parameters (UCS,  $E_{sec,50}$  and  $E_0$ ) of CT-HKMD and RCT-HKMD



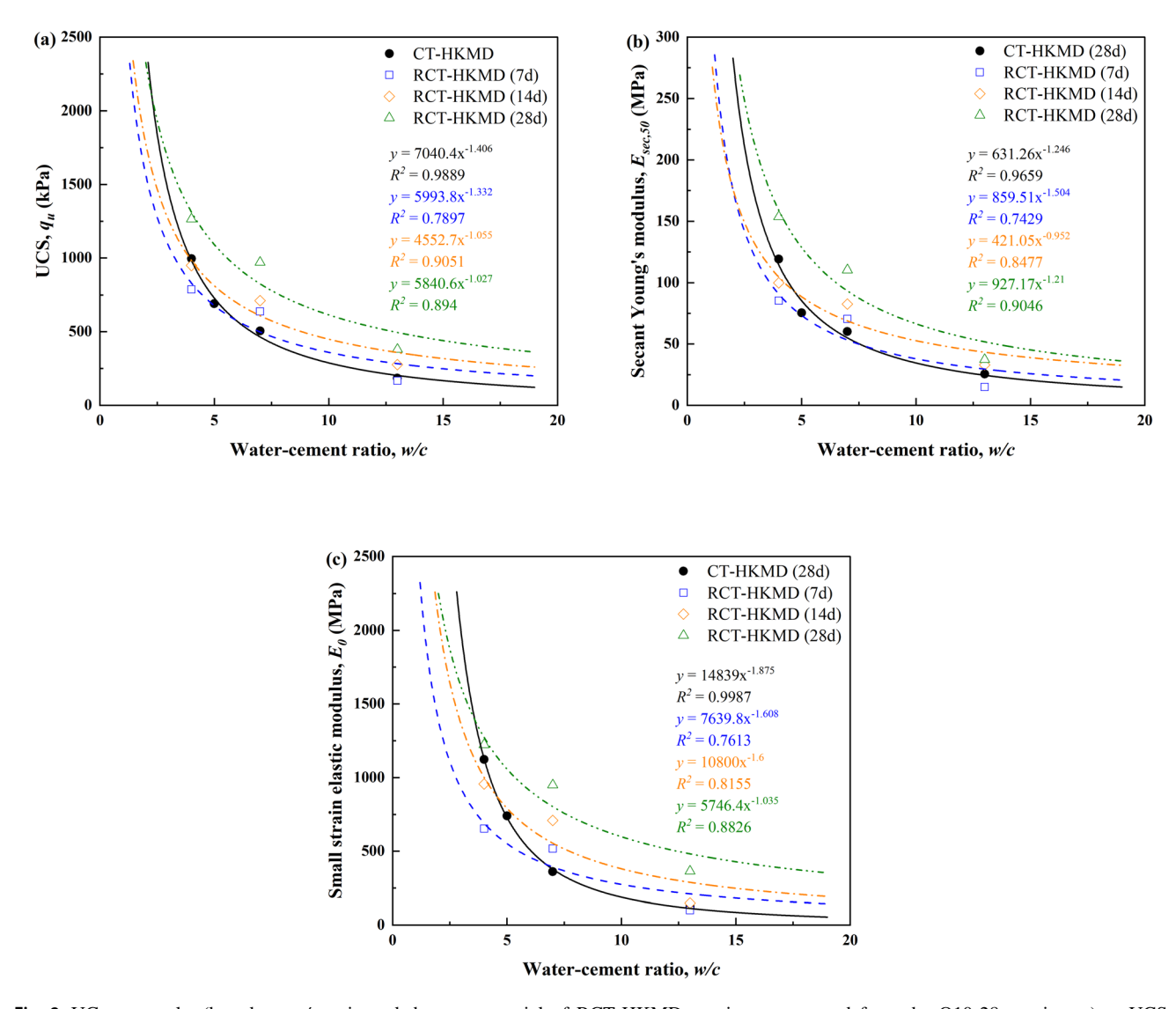


Fig. 8 UC test results (based on w/c ratio and the raw material of RCT-HKMD specimens prepared from the O10-28 specimens): **a** UCS, **b**  $E_{\text{sec},50}$  and c  $E_0$ 

specimens and the curing period, the calculated parameters and the corresponding curing period were fitted with data. As shown in Fig. 10, both UCS,  $E_{\rm sec,50}$  and  $E_0$  are dependent on the curing period. For a given cement content, UCS,  $E_{\rm sec,50}$  and  $E_0$  of CT-HKMD and RCT-HKMD specimens increase with curing period, which can be caused by more fully stabilization reactions in the specimens such as pozzolanic reaction. The cement hydration and pozzolanic reaction can proceed for months, the hydration products such as C-S-H gradually nucleate and become larger, the strength of the treated specimen can be improved over time [44].

Another aspect illustrated in Fig. 10 is the UCS,  $E_{\rm sec,50}$  and  $E_0$  show a strong power relationship, as shown below, with the curing period with high correlation coefficient, which is similar to w/c ratio. This demonstrates that the

curing period also significantly impacts UCS,  $E_{\rm sec,50}$  and  $E_0$  and can be used to simply predict the above parameters over different curing periods and raw materials in cemented soil. However, the experimental data reveal an unstable trend similar to the w/c ratio, that is, the values of a and b for cemented soil change irregularly with cement content. Consequently, these fitting equations are applicable only for a specific cement content. It is worth noting that these fitting equations are flawed, because with the increase of curing period, the hydration reaction will tend to be stable, resulting in the strength of the cemented soil also becoming stable. Hence, the fitting of the exponential equations will overestimate the UCS,  $E_{\rm sec,50}$  and  $E_0$  of the cemented soil in the longer curing period.

$$q_u$$
 or  $E_{\text{sec},50}$  or  $E_0 = a \cdot t^b$  (5)



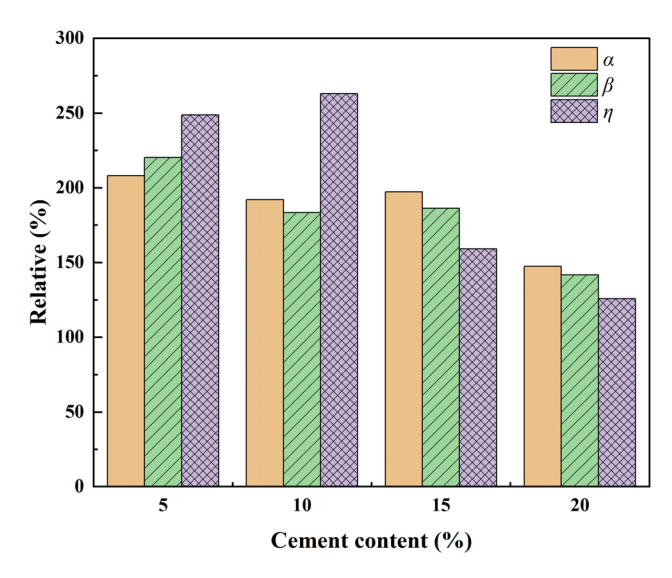


**Fig. 9** Relative results of UCS,  $E_{\text{sec},50}$  and  $E_0$ 

where  $q_u$  is the UCS,  $E_{{\rm sec},50}$  refers to the secant Young's modulus,  $E_0$  means the small strain elastic modulus, t represents the curing period, and a and b refer to experimentally fitted coefficients.

To investigate whether the  $E_{\rm sec,50}/q_u$  ratio will be affected by different raw materials in cemented soil, the calculated  $E_{\rm sec,50}/q_u$  ratio of CT-HKMD and RCT-HKMD specimens was compared as shown in Fig. 11a. The average  $E_{\rm sec,50}/q_u$  ratio of CT-HKMD specimen, which is 117, is nearly identical to that of RCT-HKMD specimen, which is 112.3. Both values are much closed to 125.1 provided by Ho et al. [25]. This suggests that the  $E_{\rm sec,50}/q_u$  ratio of cement-treated HKMD is consistently around 120, regardless of variations in cement content, curing period or cemented history. Comparing to the  $E_{\rm sec,50}/q_u$  ratio of cement-treated clay from different Asian countries, including the results from Singapore [36] and Thailand [44], the  $E_{\rm sec,50}/q_u$  ratios of cement-treated HKMD are smaller than 140 and 147, respectively, which can be

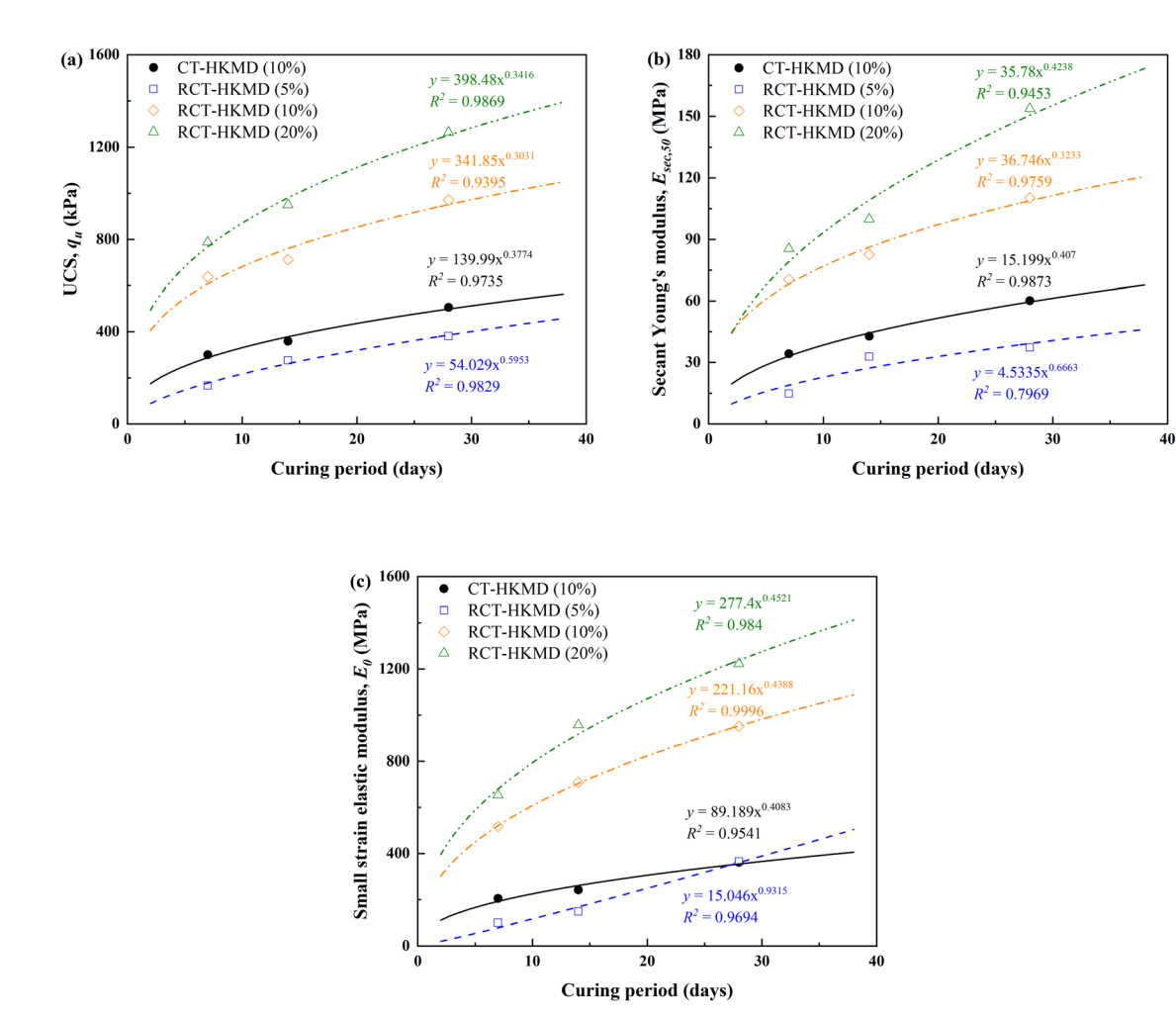


Fig. 10 UC test results (based on curing period): a UCS, b  $E_{\text{sec},50}$  and c  $E_0$ 



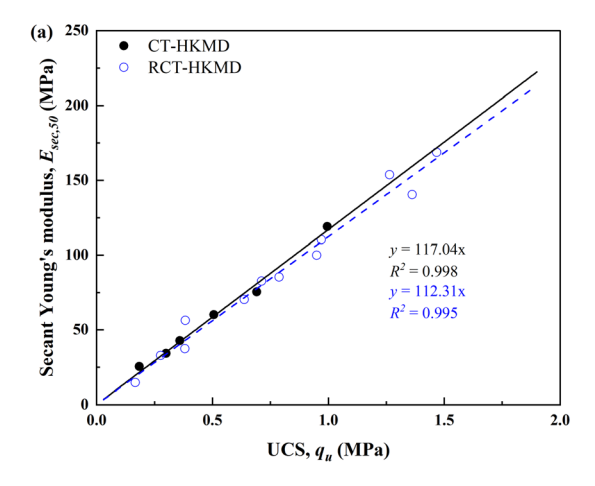


Fig. 11 Relationship between modulus and UCS: a  $E_{\text{sec},50}$  and b  $E_0$ 

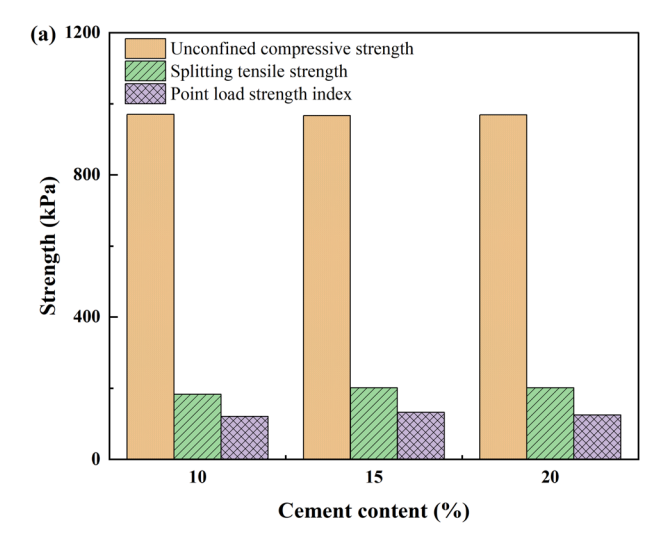
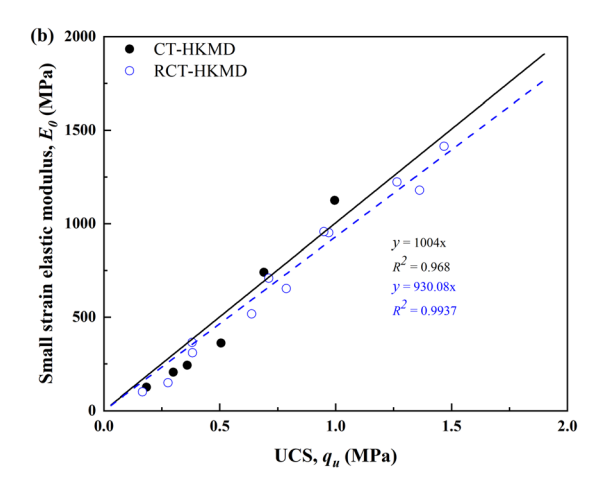
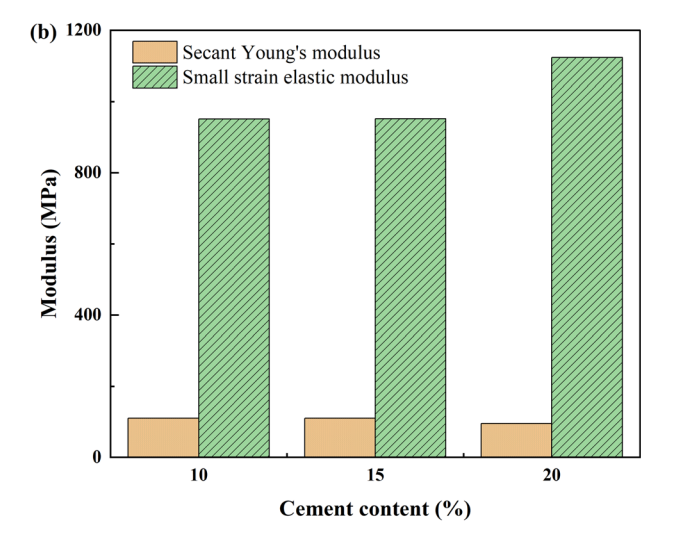


Fig. 12 Effect of cemented history: a strength and b modulus

caused by different particle size distribution. In detail, the clay content of Singapore marine clay and Bangkok clay is higher (around 68%) than that of HKMD (around 13%). After cement treatment, Singapore marine clay and Bangkok clay will be denser than HKMD and cement-treated Singapore marine clay and Bangkok clay specimens will become much more brittle and smaller failure strain than that of HKMD, leading to higher  $E_{\text{sec},50}/q_u$  ratio. Meanwhile, Fig. 11b presents the relationship between  $E_0$  and  $q_u$ , showing a good linear relationship that can simply figure out the  $E_0$  using  $q_u$ . This indicates  $E_0$  also has a strong relationship with UCS, and the  $E_0/q_u$  ratio is the same as the  $E_{\text{sec},50}/q_u$  ratio that will not be affected by cement content, curing period or cemented history.

Considering the effect of cemented history that is shown in Fig. 12, the UCS,  $E_{\text{sec},50}$  and  $E_0$  of RCT-HKMD specimens are almost same, indicating that cemented history





will not affect the strength of RCT-HKMD. Although hydration products can fill the pores and strengthen the interparticle connection and play a role in improving the structure and strength of cemented soil, the original structure and particle size distribution of the cemented soil would be destroyed after drying, crushing and sieving process [50]. Consequently, when newly 10% cement content was used for treatment, the strength of RCT-HKMD specimens would be almost same.

In general, whether the specimens are CT-HKMD or RCT-HKMD, only a few meet the design UCS of 1.3 MPa for DCM piles [39]. However, they can still be used as backfill materials, providing sufficient bearing capacity for construction machinery to further reinforce the foundation. In addition, the mix ratio can be adjusted to produce cemented soil with different mechanical properties to meet specific design requirements. For applications requiring



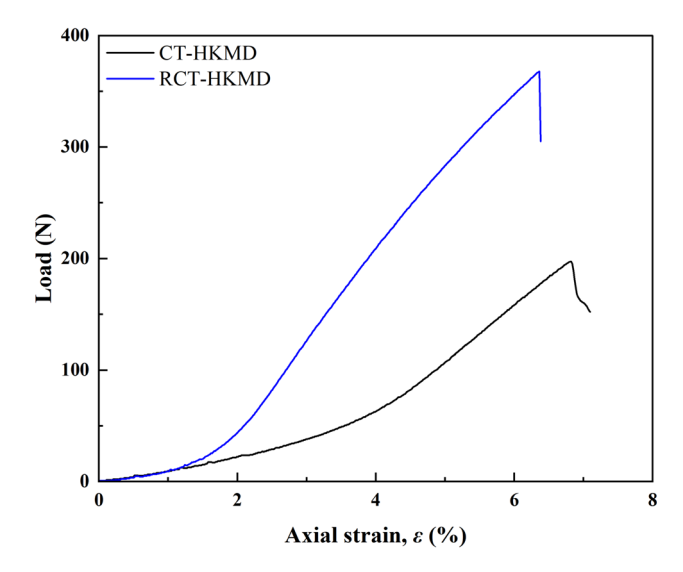


Fig. 13 A typical load-strain curve of Brazilian test of CT-HKMD and RCT-HKMD specimens

higher strength materials such as DCM, a higher cement content can be incorporated in the mix ratio.

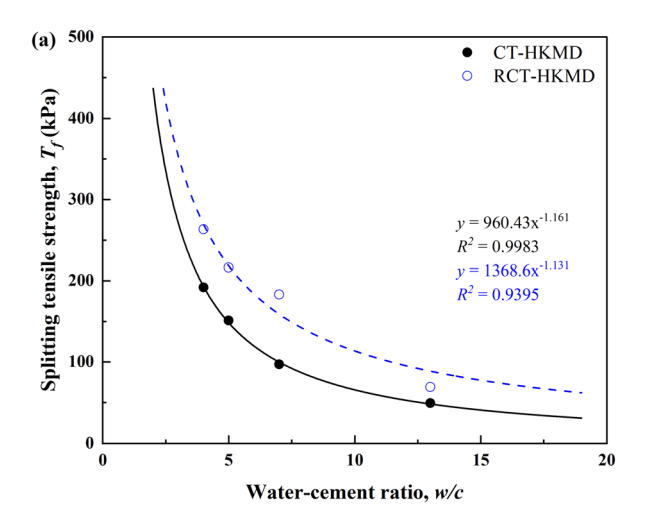
# 3.2 Splitting tensile strength

Figure 13 shows typical load–strain curve of Brazilian test of two specimens named O10-28 and O10-28-R10-28. With a similar trend to the UCS, the splitting tensile strength ( $T_f$ ) of RCT-HKMD specimen is higher than CT-HKMD specimen which can be because RCT-HKMD specimen is denser. RCT-HKMD specimen is relatively fine without large particles, and after cement treatment, the number of contacts between soil particles or clusters and cement will be greater, resulting in more hydration

products to fill the pore spaces and improve the connection between particles or clusters. Additionally, RCT-HKMD specimen shows obvious brittle characteristics because of the pore structures. The cohesion force of RCT-HKMD specimen is stronger, and as the peak load is reached, the specimen will quickly failure due to the fast formation of the fracture surface. On the other hand, the cohesion force of CT-HKMD specimen is weaker and the number of pore structures between soil particles is greater, so when the load reaches its limited, the pore structure of the specimen will be compressed that shows plastic deformation [21].

Figures 14 and 15 show the impact of the water/cement ratio and curing period on the splitting tensile strength of both types of cemented soils. As with the results of UCS, the cement content also has a significant impact on the splitting tensile strength of both types of cemented soils. Even a small addition of cement can result in a great improvement in splitting tensile strength. Besides that, the splitting tensile strength of CT-HKMD and RCT-HKMD specimens increases with decreasing water/cement ratio and increasing curing period that are consistent with general cognition which can be due to more fully hydration reaction and the detail will be explained in TG analysis. It is important to mention that the fitting equations shown in Fig. 15 are flawed since the hydration reaction tends to be stable with the increasing curing period, which in turn causes the strength of the cemented soil to be stable as well. Therefore, the fitting of the exponential equations will overestimate the splitting tensile strength of the cemented soil in the longer curing period.

To closely examine whether there is a significant difference in the splitting tensile strength between the cemented and re-cemented soil with the same water/cement



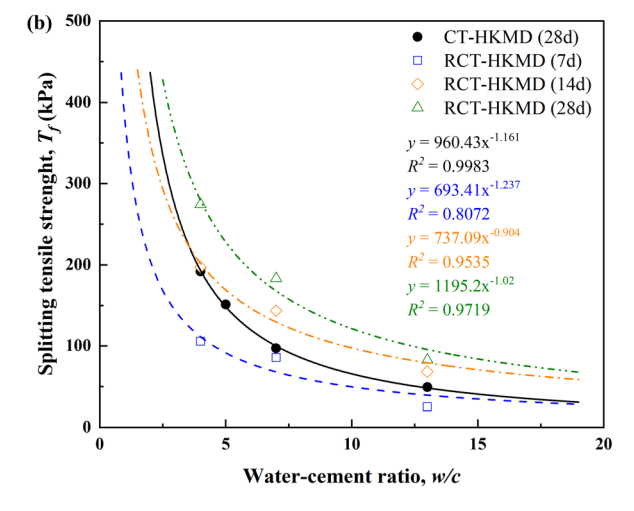


Fig. 14 Brazilian test results (based on w/c ratio): a raw material of RCT-HKMD specimens prepared from the CT-HKMD specimens with the corresponding cement content and b raw material of RCT-HKMD specimens prepared from the O10-28 specimens



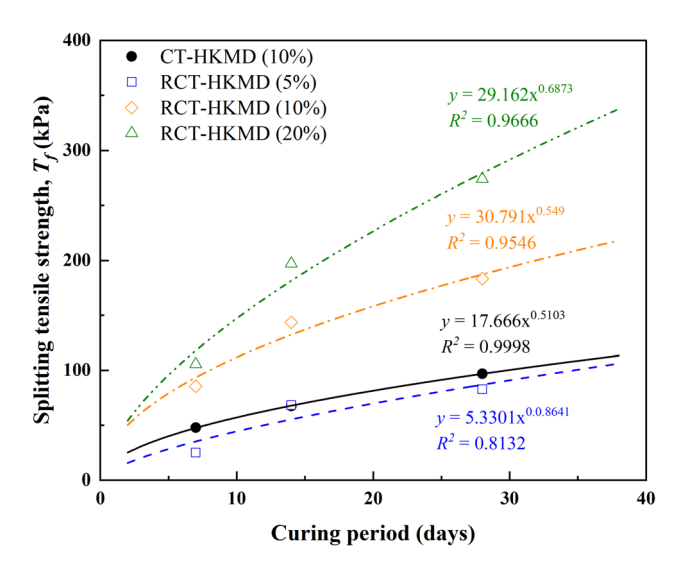


Fig. 15 Brazilian test results (based on curing period)

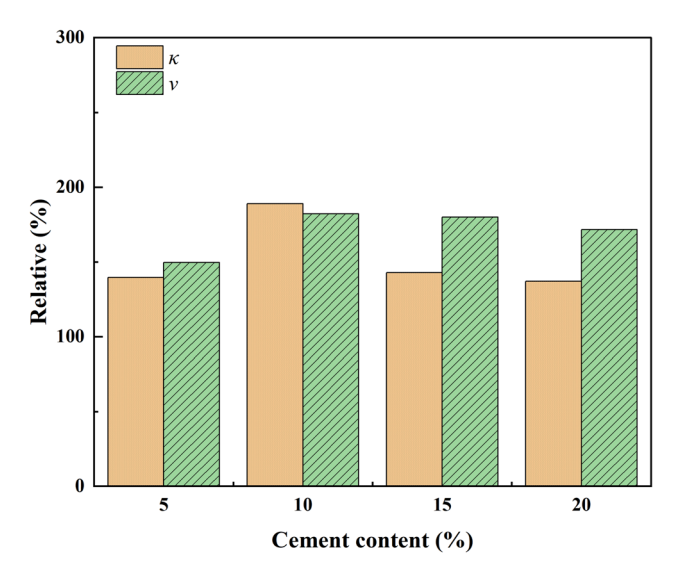


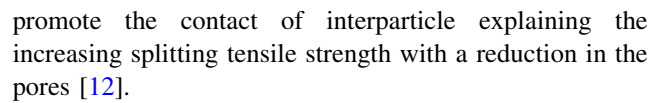
Fig. 16 Relative results of splitting tensile strength and point load strength index

ratio and curing period, their splitting tensile strengths were compared. The  $\kappa$  is calculated as follows:

$$\kappa = \frac{T_f^R}{T_f^C} \times 100\% \tag{6}$$

where  $T_f^R$  and  $T_f^C$  are the splitting tensile strength of RCT-HKMD and CT-HKMD specimens, respectively.

In detail, Fig. 16 displays the splitting tensile strength of RCT-HKMD specimen is 1.4 to 1.9 times higher than that of CT-HKMD specimen with the same content and curing period which can be explained by that the pore of RCT-HKMD specimen is small. There are no large particles in the RCT-HKMD specimen; cement can more effectively



The effect of cemented history on splitting tensile strength is also investigated as shown in Fig. 12 to understand whether cemented history affects the splitting tensile strength of re-cemented soil. The result is the same as the UC test, that is, no matter what the cemented history is, the strength of the RCT-HKMD specimens with the same cement content is almost the same.

To quantify the relationship between the splitting tensile strength of CT-HKMD and RCT-HKMD specimens and the UCS, the calculated splitting tensile strength and the corresponding UCS were fitted with data. As depicted in Fig. 17, it can be found that the best fit lines are much similar with  $0.1986q_u$  and  $0.1828q_u$ , respectively. The average is  $0.19q_u$ , which considering both CT-HKMD and RCT-HKMD specimens is little higher than  $0.132q_u$  [49] and  $0.153q_u$  [32, 57]. The results presented in this study and other studies demonstrate that the  $T_f/q_u$  ratio does not remain constant regardless of the curing period, cement content, cemented history or source of the marine clay, but can be considered to be within the range of 0.13–0.2 that has practical implications for engineers to easily predict the results of tensile strength from UCS.

## 3.3 Point load strength index

Although the differences in UCS, modulus and splitting tensile strength of cemented and re-cemented soil have been studied above, the differences in point strength index  $(I_{s(50)})$  of them will still be explored to further confirm whether the  $I_{s(50)}$  of re-cemented soil will be greatly improved compared to that of cemented soil. Figure 18a

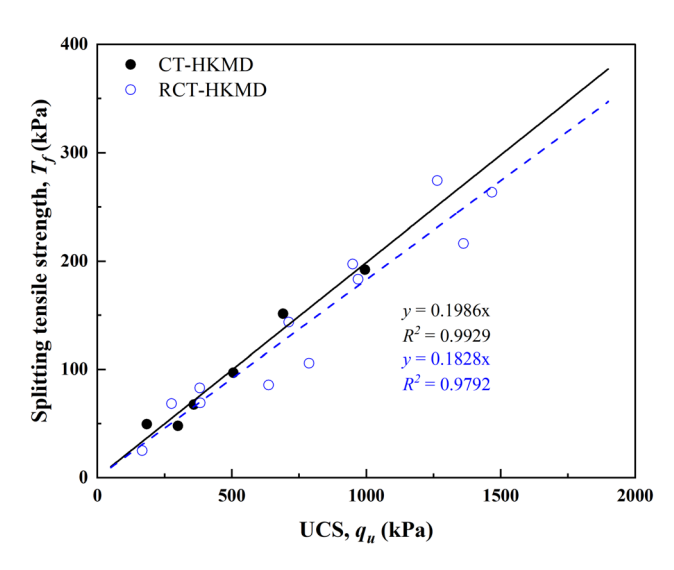


Fig. 17 Relationship between splitting tensile strength and UCS



displays the  $I_{s(50)}$  of RCT-HKMD specimen is higher than that of CT-HKMD specimen with the same cement content and curing period which is similar to UCS and splitting tensile strength results. In detail, as shown in Fig. 16, the  $I_{s(50)}$  of RCT-HKMD specimen is 1.5 to 1.8 times higher than that of CT-HKMD specimen that can be caused by the denser microstructure. Hydration products such as C-S-H can effectively improve the connection between the particles of the RCT-HKMD specimen; the  $I_{s(50)}$  will be enhanced.

The relation of  $I_{s(50)}$  with water/cement ratio and curing period suggests both in an important factor controlling  $I_{s(50)}$ that is shown in Figs. 18b and 19. It can be seen that the  $I_{s(50)}$  of CT-HKMD and RCT-HKMD specimens increases with reducing water/cement ratio and raising curing period that are consistent with general cognition that can be due to more fully hydration reaction. However, the fitting equations shown in Fig. 19 are flawed. As the curing period increases, the hydration reaction tends to be stable, which results in the strength to be stable as well. Hence, the fitting of the exponential equations will overestimate the  $I_{s(50)}$  of the cemented soil in the longer curing period. Additionally, the effect of cemented history on  $I_{s(50)}$  is explored as shown in Fig. 12. The result is same as the UC and Brazilian test, that is, no matter what the cemented history is, the strength of the RCT-HKMD specimens with the same cement content is almost the same.

Since the  $T_f$ — $I_{s(50)}$ ,  $q_u$ — $I_{s(50)}$ ,  $E_{\text{sec},50}$ -  $I_{s(50)}$  and  $E_0$ — $I_{s(50)}$  relationships of cemented soil are unclear, the corresponding parameters were fitted. The relationship between UCS, tensile strength and point load strength index is revealed in Fig. 20. All of them are in a good linear relationship with high correlation coefficients, resulting in a straightforward test method that is point load

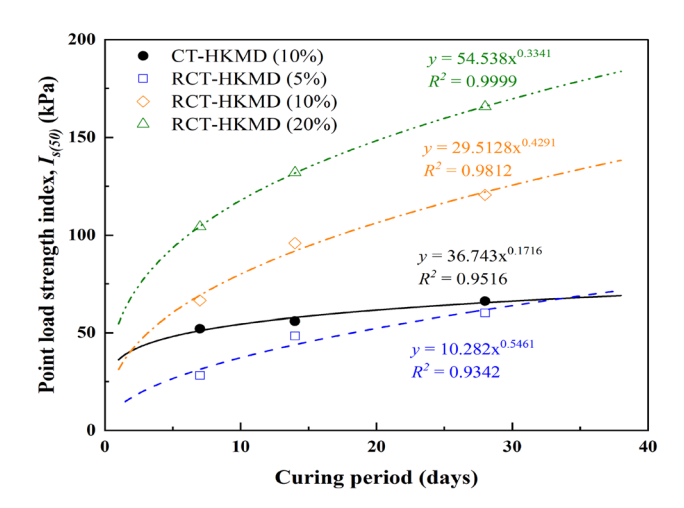
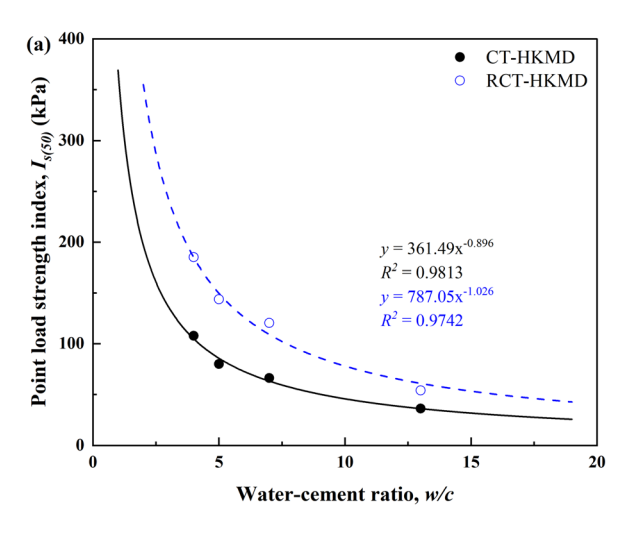


Fig. 19 Point load test results (based on curing period)

test can be used to help engineers easily estimate the strength and modulus of cemented soil to design the strength and analysis the settlement of cemented soil. Comparing with other materials, the correlation between the UCS and  $I_{s(50)}$  is 21.6 for Hong Kong granitic rocks [62] and 21.4 for mudrocks [35] and the correlation between the  $T_f$  and  $I_{s(50)}$  is 3.96 for gypsum rock [24] and 1.76 for different rocks including limestone, marble, andesite, granite and diabase [1] and both are higher than this study that can be caused by much higher strength in rock.

# 3.4 TG analysis

The TG and DTG results of HKMD and CT-HKMD and RCT-HKMD specimens with the same cement content and 28-days curing with temperature ranging from 30 to



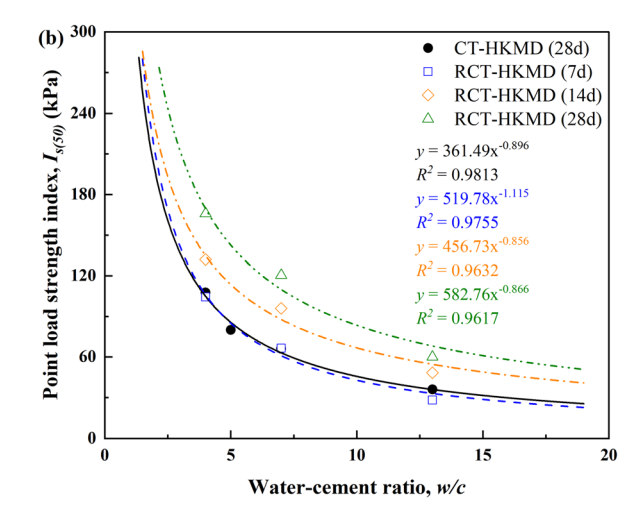


Fig. 18 Point load test results (based on w/c ratio): a raw material of RCT-HKMD specimens prepared from the CT-HKMD specimens with the corresponding cement content and b raw material of RCT-HKMD specimens prepared from the O10-28 specimens



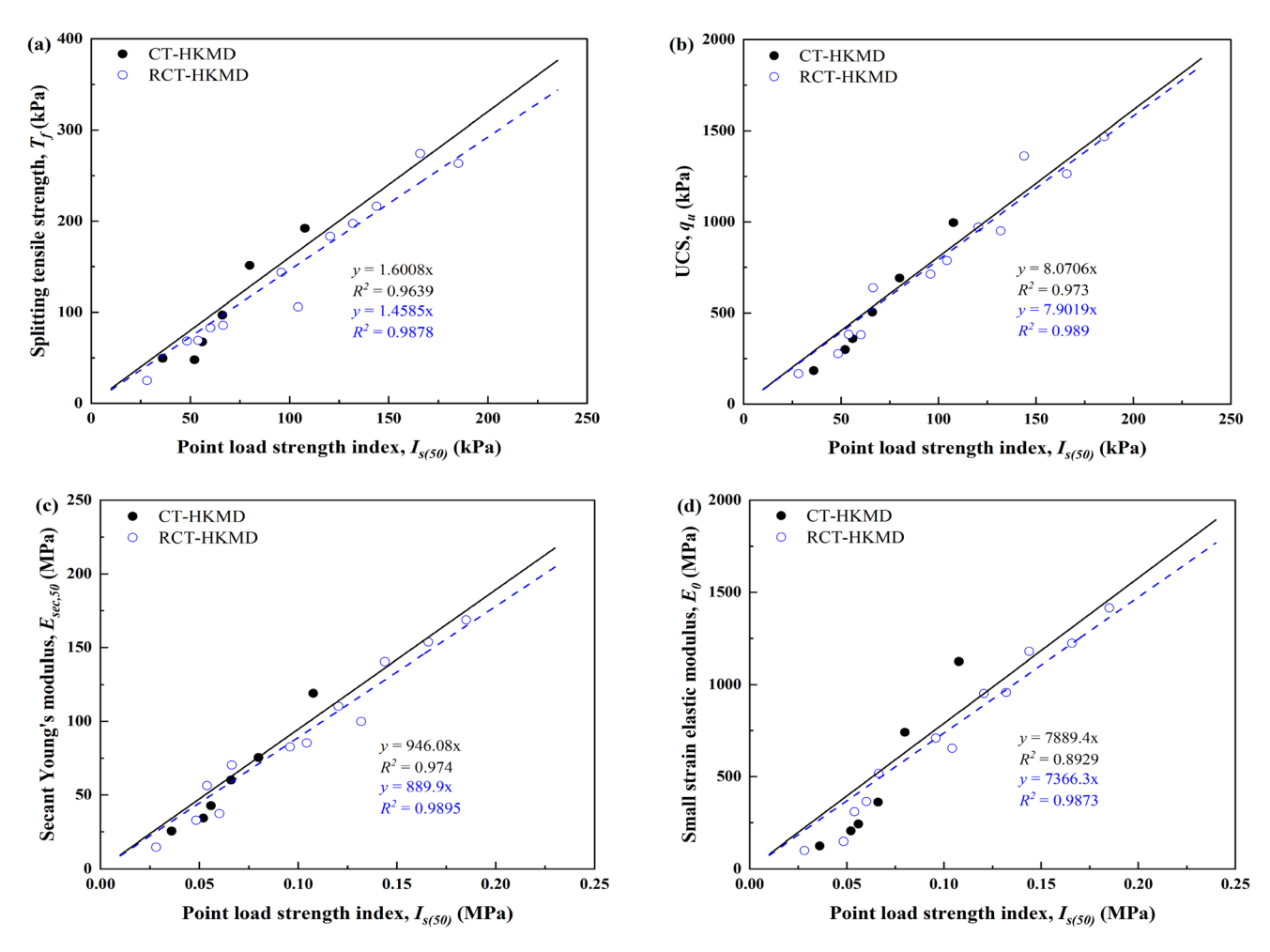


Fig. 20 Relationship between UC test, Brazilian test and point load test: a  $T_f$  versus  $I_{s(50)}$ , b  $\mathbf{q}_u$  versus  $I_{s(50)}$ , c  $E_{\text{sec},50}$  versus  $I_{s(50)}$  and d  $E_0$  versus  $I_{s(50)}$ 

900 °C are shown in Fig. 21. The total mass loss of the HKMD is 11.55%. For the CT-HKMD specimens, the mass loss increases with higher cement content, ranging from 12.6% at 5% cement content to 16.7% at 20% cement content and both are larger than 11.55%. Similarly, the RCT-HKMD specimens present the same trend but with even greater mass loss, ranging from 12.69% at 5% cement content to 22.55% at 20% cement content and both are also larger than 11.55%. This increase can be explained by the formation of more hydration products and more effective promotion of the contact of interparticle. Therefore, as has been presented, the mechanical properties of CT-HKMD and RCT-HKMD specimens will be improved with increasing cement content and the mechanical properties of RCT-HKMD specimens are better than that of CT-HKMD specimens with the same cement content and curing period.

Another feature that can also be found in Fig. 21 is the DTG curves of CT-HKMD and RCT-HKMD specimens with the same cement content and 28-day curing shows an

increase from 30 to 280 °C in the peak that corresponding to the dehydration of free water [9], clay minerals [19], C–S–H gels and ettringite [51]. For quantitative evaluation, the mass loss was calculated from the TG results that are presented in Fig. 23. With the same trend as DTG curves, mass losses also increase from 2.92 to 4.89% of CT-HKMD specimens and from 4.14 to 9.38% of RCT-HKMD specimens from 5 to 20% cement content. The results indicate that more cement hydration products including C–S–H and ettringite are formed with increasing cement content especially in RCT-HKMD specimens, so the mechanical properties of RCT-HKMD specimens are better than that of CT-HKMD specimens with the same cement content and curing period.

Another temperature ranges from 280 to 600 °C; the peak is caused by the dihydroxylation of kaolin minerals in clay [41] and Ca(OH)<sub>2</sub> crystals [22]. A slight increase in peaks as well as mass losses of CT-HKMD and RCT-HKMD specimens at these range temperatures that are



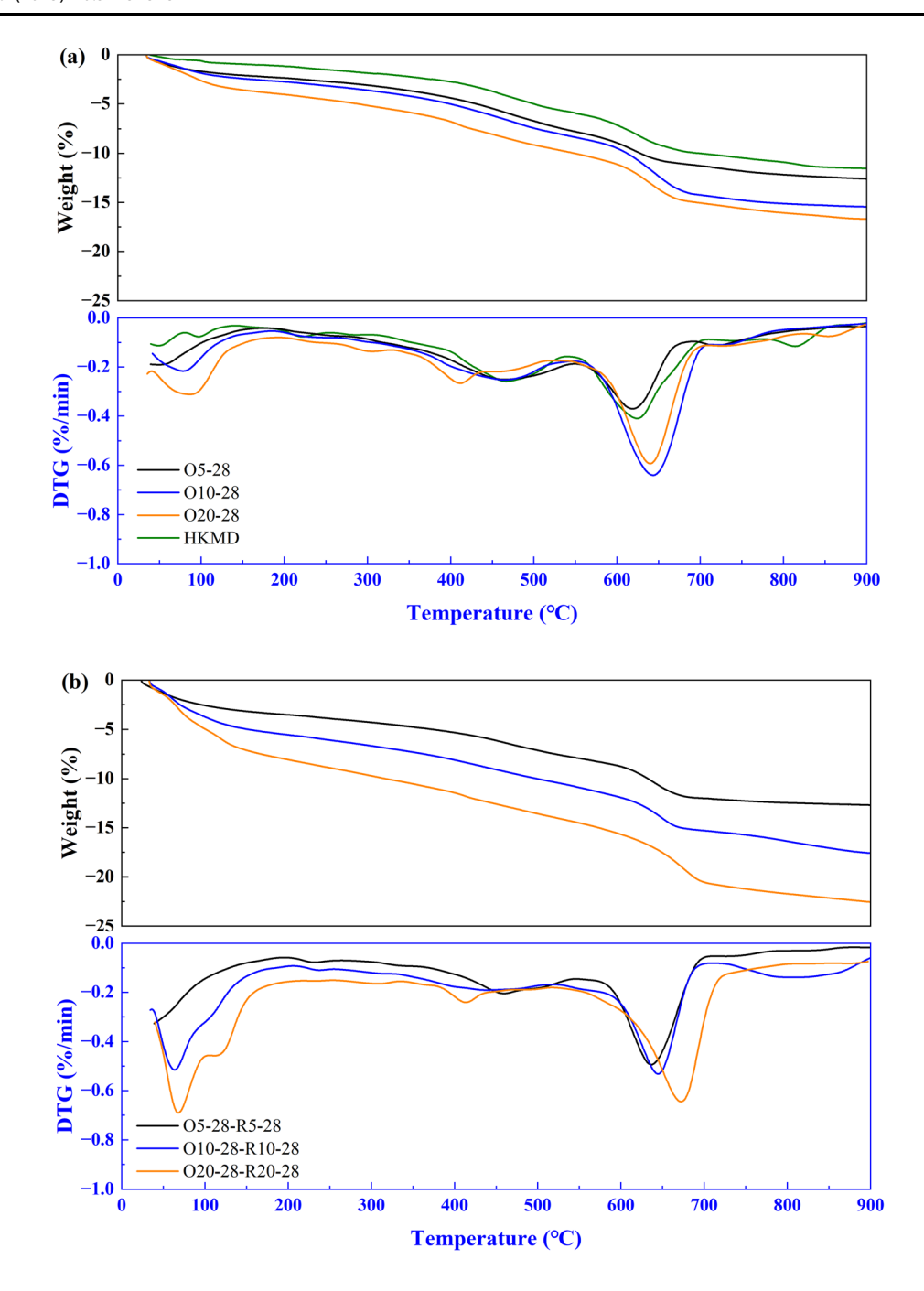


Fig. 21 TG and DTG curves: a CT-HKMD specimens and HKMD and b RCT-HKMD specimens with the raw material prepared from the CT-HKMD specimens with the corresponding cement content

related to more Ca(OH)<sub>2</sub> crystals are formed by cement content. Hence, the mechanical properties of both cemented soils will be enhanced with cement content.

The following peak between 600 and 720 °C should be contributed to the decomposition of illite, calcite and CaCO<sub>3</sub> [55, 61]. Both peak and mass loss increase with cement content of CT-HKMD and RCT-HKMD specimens

in these range of temperatures that can be caused by more CaCO<sub>3</sub> are produced for CT-HKMD specimens and more calcite existed for RCT-HKMD specimens with increasing cement content. This will also result in better mechanical properties of CT-HKMD and RCT-HKMD specimens with cement content. For CT-HKMD specimens, although cement hydration reaction has started rapidly, the large



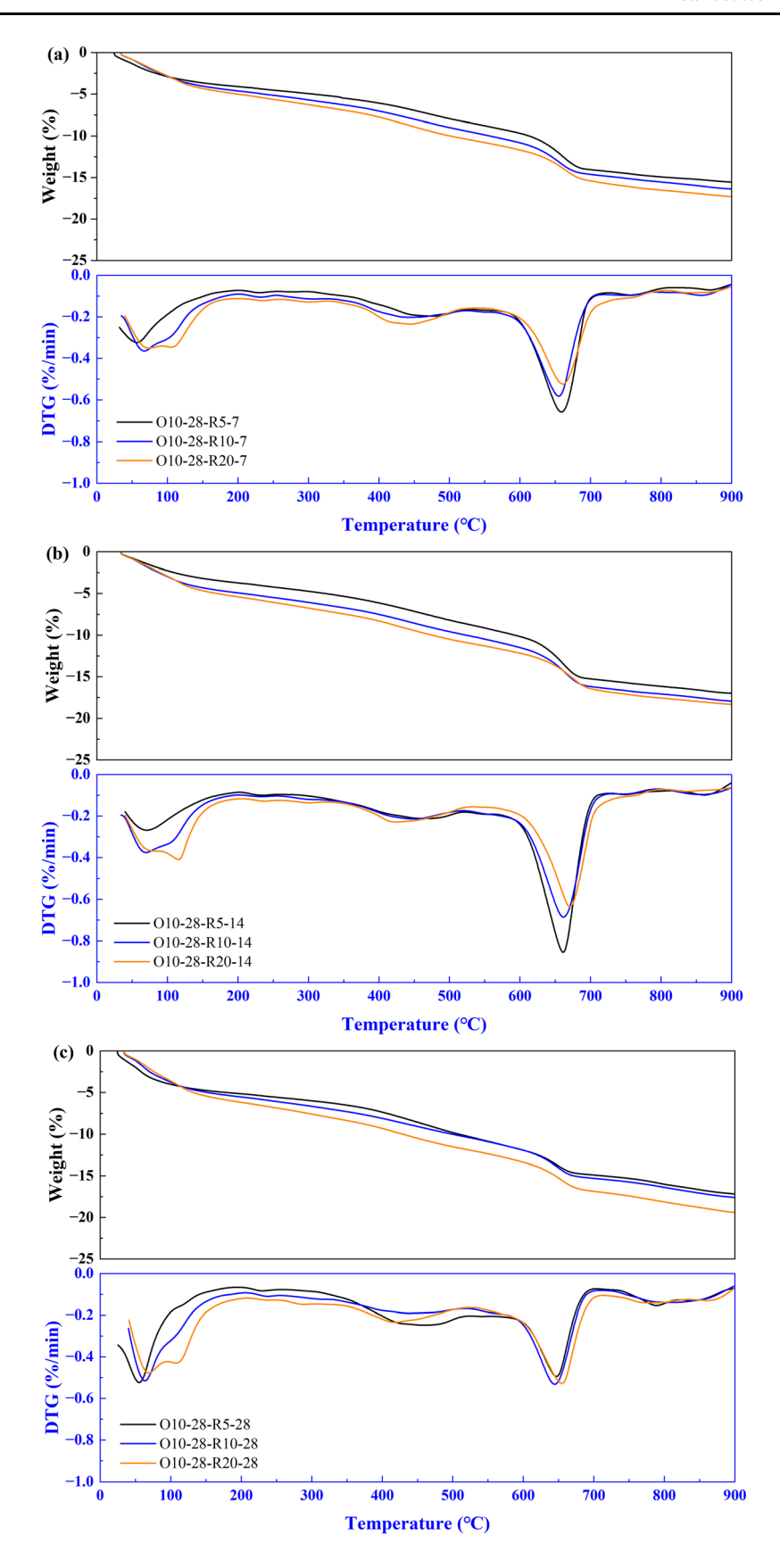
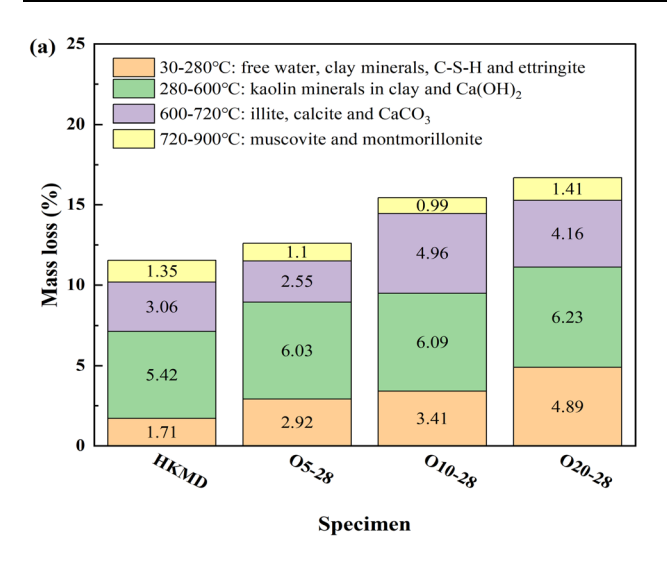


Fig. 22 TG and DTG curves of RCT-HKMD specimens: a 7-day curing, b 14-day curing and c 28-day curing





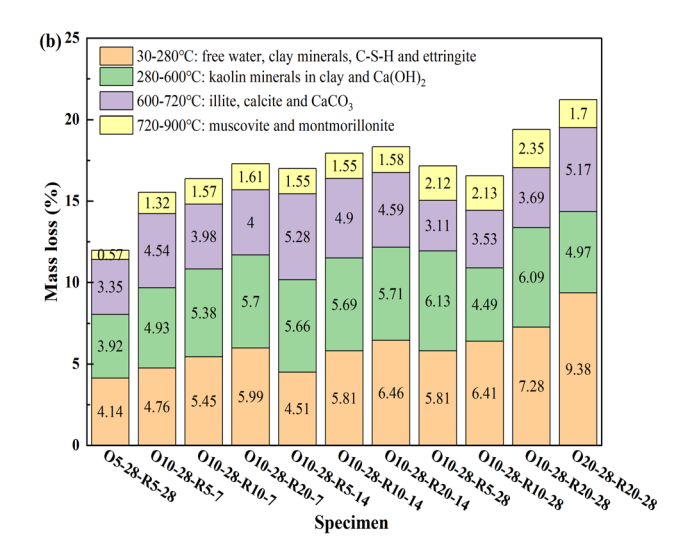


Fig. 23 Mass loss results: a HKMD and CT-HKMD specimens and b RCT-HKMD specimens

pores present during specimen preparation process prevent the hydration products from completely filling the pores in a short time. As a result, CO<sub>2</sub> can penetrate the pores and react with CaO to generate CaCO<sub>3</sub>. Regarding RCT-HKMD specimens, even though cement hydration reaction quickly happened to form hydration products to fill the small pores that can reduce the contact with CO<sub>2</sub>, the content of calcite of RCT-HKMD specimens increased with the cement content of the raw material. The raw material of RCT-HKMD specimens prepared from CT-HKMD specimens with different cement content would lead to different content of calcite. The dihydroxylation of muscovite and montmorillonite takes place between 720 and 900 °C [7, 55].

Figures 22 and 23b show the TG and DTG curves and mass loss of RCT-HKMD specimens with different cement content and curing period that the raw material of RCT-HKMD specimens was prepared from the O10-28 specimens. Consistent with other studies [43], as cement content and curing period increase, the greater content of hydration products explains the greater total mass loss in TG curves as well as the more significant peak at the temperature range from 30 to 280 °C and 280-600 °C in the DTG curves. This explains why the mechanical properties of CT-HKMD and RCT-HKMD specimens improve with cement content and curing period. However, the peak between 600 and 720 °C decreases from DTG curves with increasing cement content of 7 and 14-day curing that may be due to the reduction in contact with CO<sub>2</sub> that explains before. As shown in Fig. 22c, the peak between 600 and 720 °C decreases from DTG curves with increasing cement content of 28-day curing except 5% cement content that can be contributed to curing period that is long enough and almost all the cements participate in the hydration reaction,

resulting in a reduction in the gypsum content in the cement. It will lead to  $C_4AH_{13}$  which is one of the hydration products to react with AFt to form AFm [48]. This has been confirmed that the peak between 40 and 280 °C of O10-28-R5-28 specimen is the most conspicuous.

#### 3.5 SEM-EDS characterization

The SEM photographs of CT-HKMD specimens with 10% and 20% cement content at 28 days of curing are shown in Fig. 24. It is evident that an increase in cement content leads to denser microstructure. As a result, the mechanical properties of CT-HKMD specimens strengthen with cement content. In detail, as shown in Fig. 24a and b, the flat clay particles are arranged in a scattered pattern and exhibit some reticulation in an open type of microstructure caused by low cement content. Due to the hydration products, which are detected as C-S-H (or C-A-S-H) and ettringite (AFt) by EDS methods, these will form in reticular structure. Additionally, plate-like portlandite (CH) is also discovered from EDS with high concentration of Ca and low concentration of Si and Al [63]. The flocculated nature of the structure with clusters of treated clay particles distributed around large openings becomes more noticeable and improves bonds among soil particles with increasing cement content (Fig. 24c and d) which can be caused by the cation exchange process with Ca<sup>2+</sup> cations replacing Na<sup>+</sup> or K<sup>+</sup> cations [37]. Simultaneously, the degree of reticulation seems to rise, and the flatness of the structure becomes less noticeable. As can be seen, fine reticulation becomes quite noticeable at 20% cement content (Fig. 24c and d). The rise in C-S-H/C-A-S-H gels and ettringite (AFt) mixed with C-(A)-S-H that show reticular in



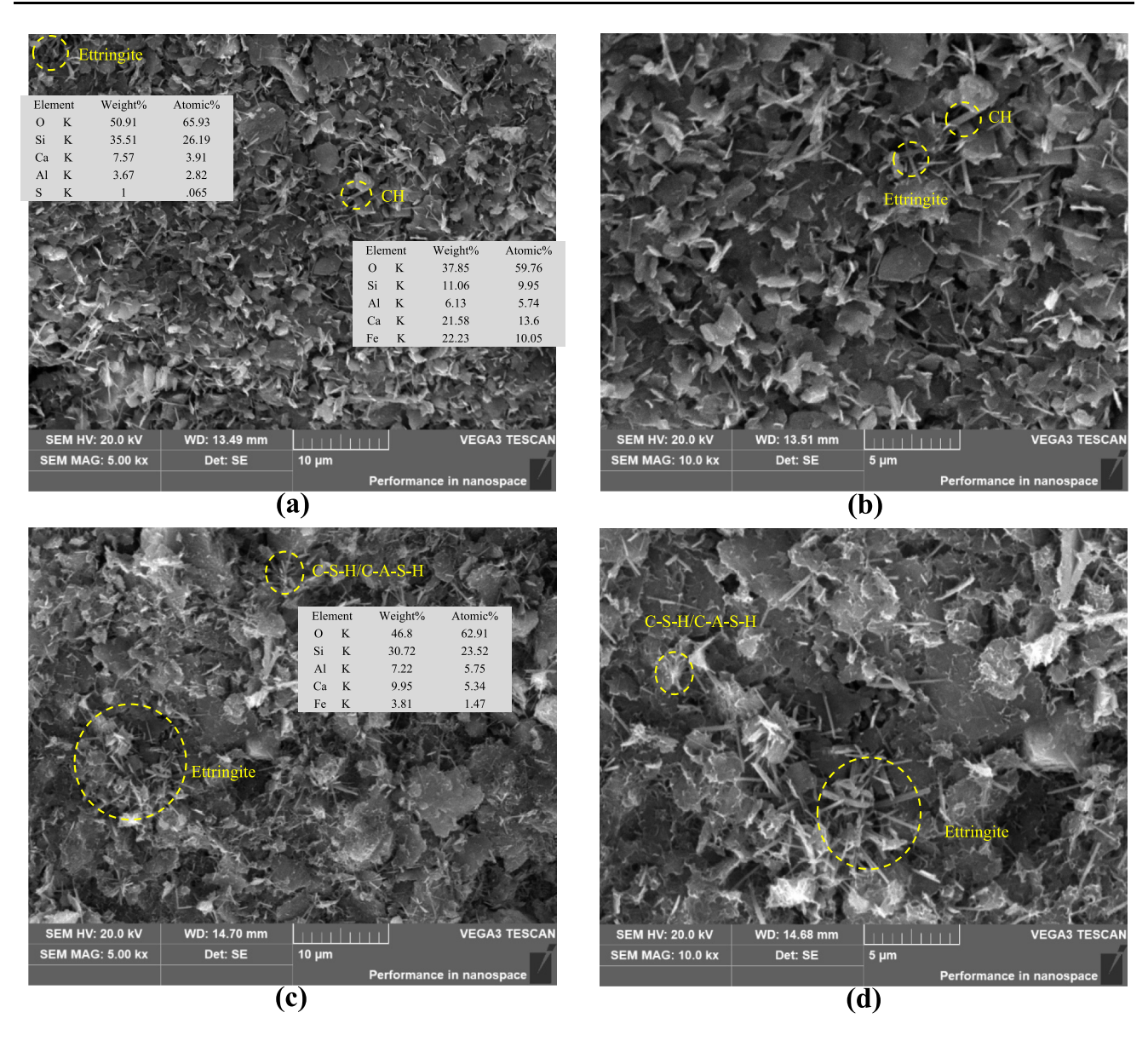


Fig. 24 SEM images of CT-HKMD specimens: a O10-28-5 kx, b O10-28-10 kx, c O20-28-5 kx and d O20-28-10 kx

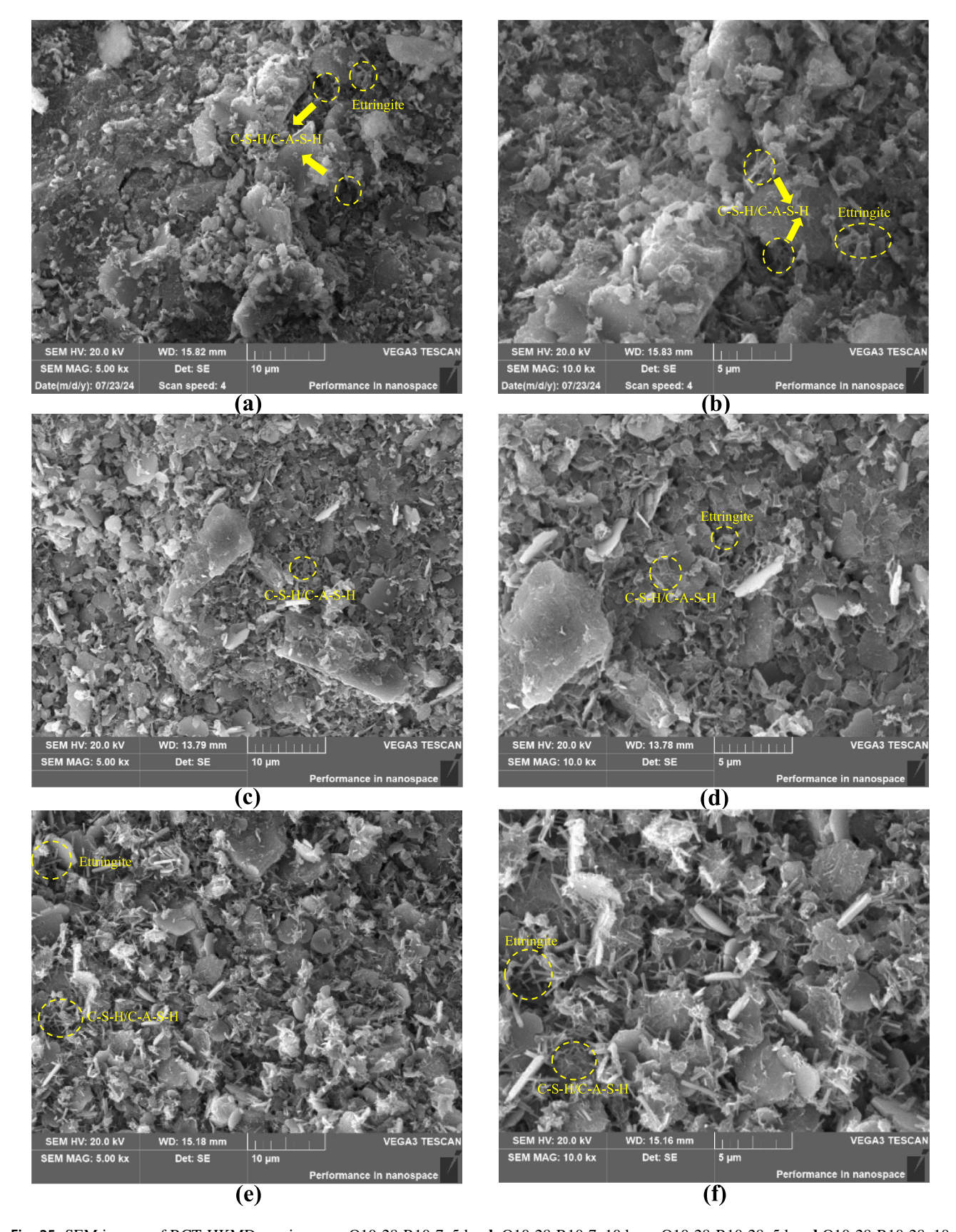
structure and needle-like or fibrillar morphology is responsible for the increase in the degree of reticulation [31]. These hydration products are detected by EDS which is in agreement with the results presented by Sun et al. [55].

The SEM images of RCT-HKMD specimens with 10% cement content at 7 and 28 days of curing and 20% cement content at 28 days of curing are shown in Fig. 25. The results are also the same as those of CT-HKMD specimens that the microstructure is much denser with increasing cement content because of the increase in hydration products. At the same time, as the cement content increases, a more obvious flocculated nature of the structure will be found, and hydration products are clearer to be seen. In addition, compared to the SEM images of CT-HKMD specimens shown in Fig. 24, RCT-HKMD specimens

present a much denser microstructure because there are no coarse particles inside the RCT-HKMD specimen and have a greater number of contacts between soil particles; the hydration reaction will be more intense, which results in more hydration products such as C–S–H and C–A–S–H. These hydration products can not only improve the bonding strength between particles or clusters, but also fill the pore space so that the mechanical property of RCT-HKMD specimen is better than that of CT-HKMD specimen.

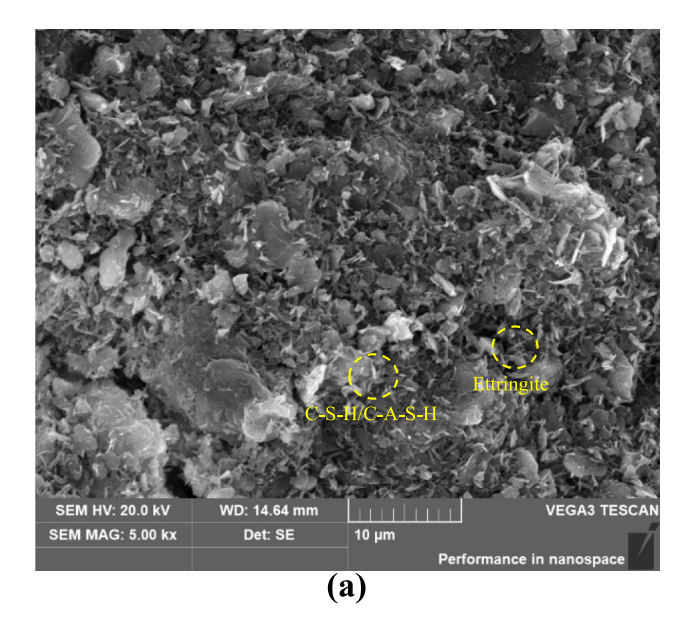
Figure 25 also shows the SEM photographs of RCT-HKMD specimens at different curing periods. Over time, hydration products are clearly visible such as ettringite and C–S–H gels as well as the microstructure becomes denser and more flocculated as the hydration products grow over time. As a consequence, the mechanical properties of





**Fig. 25** SEM images of RCT-HKMD specimens: **a** O10-28-R10-7–5 kx, **b** O10-28-R10-7–10 kx, **c** O10-28-R10-28–5 kx, **d** O10-28-R10-28–10 kx, **e** O10-28-R20-28–5 kx and **f** O10-28-R20-28–10 kx





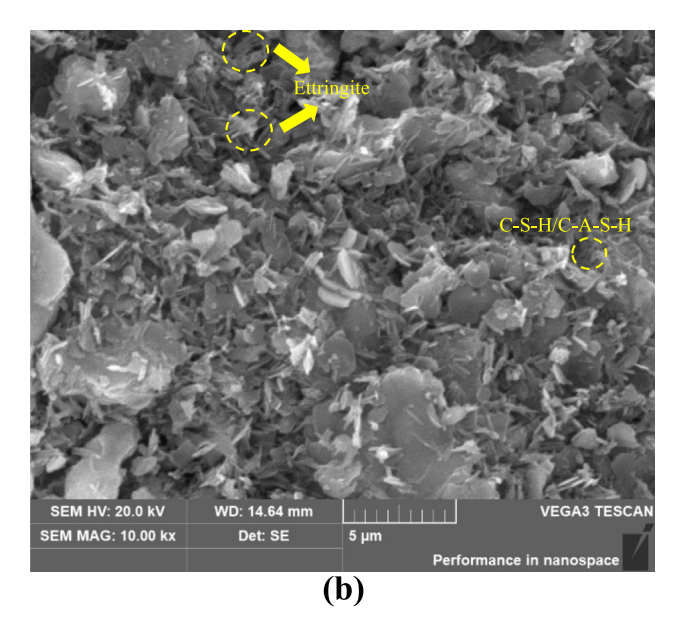


Fig. 26 SEM images of O20-28-R10-28 specimens: a 5 kx and b 10 kx

cemented soil will be improved with curing period. In detail, the hydration reaction will quickly form ettringite (AFt), C-(A)-S-H and so on and the hydration rate is fast and then over time, these hydration products gradually nucleate and grow and the hydration rate is gradually decreased, while the hydration rate at this time is mainly controlled by diffusion [10]. Additionally, Figs. 25c, d and 26 present the SEM photographs of RCT-HKMD specimens that consider the effect of cemented history. It can be found that the microstructures are much similar with relatively dense structures. This is also familiar with the results discussed before, that is, the cemented history will not affect the mechanical property of cemented soil. Hence, the cemented history has no effect on RCT-HKMD specimens.

#### 4 Conclusions

A series of tests, including unconfined compression test, Brazilian test and point load test, were conducted for investigating the mechanic properties of cemented HKMD and re-cemented HKMD. Furthermore, microstructures of these cemented soils were analysis through SEM and TG tests. Based on the test results, the following conclusions can be drawn:

 The cemented history does not have influence on the re-cemented soft soils, because crush and sieve had broken the microstructures of the original cemented soils. Therefore, the cemented history can be neglected for the beneficial reuse of recycled cemented soils.

- 2. The re-cemented HKMD possessed the higher values of UCS,  $E_0$ ,  $E_{\text{sec},50}$ , splitting tensile strength and point load strength index compared to cemented HKMD with the same cement content and curing period due to greater number of contacts between soil particles or clusters and cement which can improve the interparticle bonding and filling effect of pore space to form more hydration products and denser microstructure.
- 3. The empirical equations proposed in this report, the UCS,  $E_0$ ,  $E_{\text{sec},50}$ , splitting tensile strength and point load strength index under different w/c ratios and curing periods can be predicted. In addition, there is a good linear relationship between point load strength index and UCS,  $E_0$ ,  $E_{\text{sec},50}$  and splitting tensile strength. All empirical equations recommended in this study are of practical value to engineering practitioners in designing cemented soil strength and analyzing settlement.

Acknowledgements This research was supported by the Research Grants Council of Hong Kong Special Administrative Region Government of China (Grant No. 15227923), the Research Centre for Resources Engineering Towards Carbon Neutrality (RCRE) of The Hong Kong Polytechnic University (No. 1-BBEM), and the Natural Science Foundation of Guangdong Province of The Foshan University (Grant No. 2023A1515011772). The authors also acknowledge the financial support from grant (BDT3) from the Research Institute for Land and Space of The Hong Kong Polytechnic University. This support is gratefully acknowledged.

Author contributions Wei-Feng HUANG performed data curation, formal analysis, investigation, and writing—original draft. Zhi-Jian Ruan presented methodology and investigation. Dian-Long Wang and Ma-Yao Cheng provided methodology, resources and supervision.



Ding-Bao Song offered funding acquisition, project administration, writing—review and editing. All authors reviewed the manuscript.

Funding Open access funding provided by The Hong Kong Polytechnic University.

Data availability Data will be made available on reasonable request.

#### **Declarations**

Conflict of interest The authors declare no conflict of interest.

Open Access This article is licensed under a Creative Commons Attribution 4.0 International License, which permits use, sharing, adaptation, distribution and reproduction in any medium or format, as long as you give appropriate credit to the original author(s) and the source, provide a link to the Creative Commons licence, and indicate if changes were made. The images or other third party material in this article are included in the article's Creative Commons licence, unless indicated otherwise in a credit line to the material. If material is not included in the article's Creative Commons licence and your intended use is not permitted by statutory regulation or exceeds the permitted use, you will need to obtain permission directly from the copyright holder. To view a copy of this licence, visit http://creativecommons.org/licenses/by/4.0/.

# References

- Akbay D, Altindag R (2020) Reliability and evaluation of point load index values obtained from different testing devices. J South Afr Inst Min Metall 120:181–190. https://doi.org/10.17159/2411-9717/759/2020
- ASTM (2008) Standard test method for determination of the point load strength index of rock and application to rock strength classifications (ASTM D5731). American Society for Testing and Materials, West Conshohocken
- ASTM (2016) Standard test method for unconfined compressive strength of cohesive soil (ASTM D2166). American Society for Testing and Materials, West Conshohocken
- ASTM (2017) Standard test method for splitting tensile strength of cylindrical concrete specimens (ASTM C496/C496M).
   American Society for Testing and Materials, West Conshohocken
- Baldovino JdJA, Izzo RLdS, Silva ÉRd, Rose JL (2020) Sustainable use of recycled-glass powder in soil stabilization. J Mater Civ Eng 32(5):04020080. https://doi.org/10.1061/(ASCE)MT. 1943-5533.0003081
- Bhadriraju V, Puppala AJ, Madhyannapu RS, Williammee R (2008) Laboratory procedure to obtain well-mixed soil binder samples of medium stiff to stiff expansive clayey soil for deep soil mixing simulation. Geotech Test J 31(3):225–238. https:// doi.org/10.1520/GTJ100936
- Bouras F, Al-Mukhtar M, Tapsoba N, Belayachi N, Sabio S, Beck K, Martin M (2022) Geotechnical behavior and physico-chemical changes of lime-treated and cement-treated silty soil. Geotech Geol Eng 40(4):2033–2049. https://doi.org/10.1007/s10706-021-02008-2
- British Standards Institution (1990) British standard methods of test for soils for civil engine-ering purposes. British Standards Institution, London
- 9. Bui H, Boutouil M, Levacher D, Sebaibi N (2021) Evaluation of the influence of accelerated carbonation on the microstructure and mechanical characteristics of coconut fibre-reinforced

- cementitious matrix. J Build Eng 39:102269. https://doi.org/10.1016/j.jobe.2021.102269
- Bullard JW, Jennings HM, Livingston RA, Nonat A, Scherer GW, Schweitzer JS, Scrivener KL, Thomas JJ (2011) Mechanisms of cement hydration. Cem Concr Res 41(12):1208–1223. https://doi.org/10.1016/j.cemconres.2010.09.011
- Cardoso R, Silva RV, de Brito J, Dhir R (2016) Use of recycled aggregates from construction and demolition waste in geotechnical applications: a literature review. Waste Manag 49:131–145. https://doi.org/10.1016/j.wasman.2015.12.021
- Chang TS, Woods RD (1992) Effect of particle contact bond on shear modulus. J Geotech Eng 118(8):1216–1233. https://doi.org/ 10.1061/(ASCE)0733-9410(1992)118:8(1216)
- Chiu C, Zhu W, Zhang C (2009) Yielding and shear behaviour of cement-treated dredged materials. Eng Geol 103(1–2):1–12. https://doi.org/10.1016/j.enggeo.2008.07.007
- Clough GW, Sitar N, Bachus RC, Rad NS (1981) Cemented sands under static loading. J Geotech Eng Div 107(6):799–817. https://doi.org/10.1061/AJGEB6.0001152
- Dai J, He J, Wang Q, Lou X (2024) Effects of the water-cement ratio and the molding temperature on the hydration heat of cement. J Wuhan Univ Technol Mater Sci Ed 39(4):990–998. https://doi.org/10.1007/s11595-024-2962-y
- Denies N, Huybrechts N, De Cock F, Lameire B, Maertens J, Vervoort A (2012) Soil mix walls as retaining structures-Belgian practice III-83. In: Proceedings GI. Brussels, Belgium.
- 17. Feng WQ, Bayat M, Bin L, Mousavi Z, Lin JF, Li AG (2024) Shear strength enhancement in soil using polyurethane foam adhesive and cement injections. Int J Geosynth Ground Eng 10(6):97. https://doi.org/10.1007/s40891-024-00603-w
- Feng WQ, Lalit B, Yin ZY, Yin JH (2017) Long-term non-linear creep and swelling behavior of Hong Kong marine deposits in oedometer condition. Comput Geotech 84:1–15. https://doi.org/ 10.1016/j.compgeo.2016.11.009
- Fernandez R, Martirena F, Scrivener KL (2011) The origin of the pozzolanic activity of calcined clay minerals: a comparison between kaolinite, illite and montmorillonite. Cem Concr Res 41(1):113–122. https://doi.org/10.1016/j.cemconres.2010.09.013
- Ge S, Pan Y, Zheng L, Xie X (2020) Effects of organic matter components and incubation on the cement-based stabilization/solidification characteristics of lead-contaminated soil. Chemosphere 260:127646. https://doi.org/10.1016/j.chemo sphere.2020.127646
- Geng K, Chai J, Qin Y, Xu Z, Cao J, Zhou H, Zhang X (2023)
   Damage evolution, brittleness and solidification mechanism of cement soil and alkali-activated slag soil. J Market Res 25:6039–6060. https://doi.org/10.1016/j.jmrt.2023.07.087
- He X, Chen Y, Tan X, Wang S, Liu L (2020) Determining the water content and void ratio of cement-treated dredged soil from the hydration degree of cement. Eng Geol 279:105892. https:// doi.org/10.1016/j.enggeo.2020.105892
- He SH, Yin ZY, Ding Z, Li RD (2024) Particle morphology and principal stress direction dependent strength anisotropy through torsional shear testing. Can Geotech J. https://doi.org/10.1139/ cgj-2023-0717
- Heidari M, Khanlari GR, Torabi Kaveh M, Kargarian S (2012) Predicting the uniaxial compressive and tensile strengths of gypsum rock by point load testing. Rock Mech Rock Eng 45(2):265–273. https://doi.org/10.1007/s00603-011-0196-8
- Ho TO, Chen WB, Yin JH, Wu PC, Tsang DC (2021) Stress-strain behaviour of cement-stabilized Hong Kong marine deposits. Constr Build Mater 274:122103. https://doi.org/10.1016/j.conbuildmat.2020.122103
- 26. Ho TO, Tsang DC, Chen WB, Yin JH (2020) Evaluating the environmental impact of contaminated sediment column



- stabilized by deep cement mixing. Chemosphere 261:127755. https://doi.org/10.1016/j.chemosphere.2020.127755
- Horpibulsuk S, Chinkulkijniwat A, Cholphatsorn A, Suebsuk J, Liu MD (2012) Consolidation behavior of soil-cement column improved ground. Comput Geotech 43:37–50. https://doi.org/10. 1016/j.compgeo.2012.02.003
- Horpibulsuk S, Miura N, Bergado DT (2004) Undrained shear behavior of cement admixed clay at high water content.
   J Geotech Geoenviron Eng 130(10):1096–1105. https://doi.org/ 10.1061/(ASCE)1090-0241(2004)130:10(1096)
- Horpibulsuk S, Miura N, Nagaraj TS (2003) Assessment of strength development in cement-admixed high water content clays with Abrams' law as a basis. Géotechnique 53(4):439–444. https://doi.org/10.1680/geot.2003.53.4.439
- Huawen X (2009) Yielding and failure of cement treated soil.
   National University of Singapore, Singapore
- Kamruzzaman AH, Chew SH, Lee FH (2009) Structuration and destructuration behavior of cement-treated Singapore marine clay. J Geotech Geoenviron Eng 135(4):573–589. https://doi.org/ 10.1061/(ASCE)1090-0241(2009)135:4(573)
- Kanda T, Tanaka S, Nohara H, Kubota J (1999) Development of high-performance fiber-reinforced soil cement. Annu Rep Kajima Tech Res Inst 47:79–85
- Kitazume M, Terashi M (2013) The deep mixing method. CRC Press. https://doi.org/10.1201/b13873
- 34. Komurlu E, Kesimal A, Demir S (2015) Experimental and numerical study on determination of indirect (splitting) tensile strength of rocks under various load apparatus. Can Geotech J 53(2):360–372. https://doi.org/10.1139/cgj-2014-0356
- Lashkaripour GR (2002) Predicting mechanical properties of mudrock from index parameters. Bull Eng Geol Environ 61:73–77. https://doi.org/10.1007/s100640100116
- Lee FH, Lee Y, Chew SH, Yong KY (2005) Strength and modulus of marine clay-cement mixes. J Geotech Geoenviron Eng 131(2):178–186. https://doi.org/10.1061/(ASCE)1090-0241(2005)131:2(178)
- Lei H, Qi Z, Feng S, Lei S (2022) Macroscopic and microscopic investigation of the structural characteristics of artificially structured marine clay. Soils Found 62(6):101243. https://doi.org/10. 1016/j.sandf.2022.101243
- Li Y, Eyley S, Thielemans W, Yuan Q, Li J (2022) Valorization of deep soil mixing residue in cement-based materials. Resour Conserv Recycl 187:106597. https://doi.org/10.1016/j.resconrec. 2022.106597
- Li W, Liu AS, Kwok CY, Sit CY, Shiu HK (2023) Mechanical behaviour of Hong Kong marine deposits stabilized with high content of coal fly ash. Constr Build Mater 392:131837. https:// doi.org/10.1016/j.conbuildmat.2023.131837
- Li R, Yin ZY, He SH (2025) 3D reconstruction of arbitrary granular media utilizing vision f-oundation model. Applied Soft Computing 169:112599. https://doi.org/10.1016/j.asoc.2024.1125
- Liu J, Tan Z, Zhao Q, Liu B, Wang X (2024) Mechanical properties and durability analysis of CS-CG stabilized soil: towards sustainable subgrade soil enhancement. Constr Build Mater 442:137634. https://doi.org/10.1016/j.conbuildmat.2024. 137634
- Liu Y, He LQ, Jiang YJ, Sun MM, Chen EJ, Lee FH (2019) Effect of in situ water content variation on the spatial variation of strength of deep cement-mixed clay. Géotechnique 69(5):391–405. https://doi.org/10.1680/jgeot.17.P.149
- Liu Z, Ong Dominic EL, Wang S, Oh E, Liu Y (2023) Mineralogical and microstructural characterization of cement-stabilized soft soils based on quantitative analyses. J Mater Civ Eng 35(3):04022487. https://doi.org/10.1061/(ASCE)MT.1943-5533. 0004662

- Lorenzo GA, Bergado DT (2006) Fundamental characteristics of cement-admixed clay in deep mixing. J Mater Civ Eng 18(2):161–174. https://doi.org/10.1061/(ASCE)0899-1561(2006) 18:2(161)
- 45. Moon SW, Vinoth G, Subramanian S, Kim J, Ku T (2020) Effect of fine particles on strength and stiffness of cement treated sand. Granular Matter. https://doi.org/10.1007/s10035-019-0975-6
- Nakayenga J, Cikmit AA, Tsuchida T, Hata T (2021) Influence of stone powder content and particle size on the strength of cementtreated clay. Constr Build Mater 305:124710. https://doi.org/10. 1016/j.conbuildmat.2021.124710
- 47. Navia R, Rivela B, Lorber KE, Méndez R (2006) Recycling contaminated soil as alternative raw material in cement facilities: life cycle assessment. Resour Conserv Recycl 48(4):339–356. https://doi.org/10.1016/j.resconrec.2006.01.007
- 48. Quennoz A, Scrivener KL (2012) Hydration of C3A–gypsum systems. Cem Concr Res 42(7):1032–1041. https://doi.org/10.1016/j.cemconres.2012.04.005
- Saitoh S, Suzuki Y, Nishioka S, Okumura R (1996) Required strength of improved ground. In: Grouting and deep mixing: Proc. IS Tokyo'96, 2nd Int. Conf. on Ground Improvement Geosystems 375–380.
- Sharkawi AM, Mofty SEIDM, Showaib EA, Abbass SM (2018) Feasible construction ap-plications for different sizes of recycled construction demolition wastes. Alex Eng J 57(4):3351–3366. https://doi.org/10.1016/j.aej.2017.11.014
- 51. Shen P, Lu L, He Y, Wang F, Hu S (2017) Hydration of quaternary phase-gypsum system. Constr Build Mater 152:145–153. https://doi.org/10.1016/j.conbuildmat.2017.06.179
- Song DB, Chen WB, Yin ZY, Song SX, Yin JH (2023) Recycling dredged mud slurry using vacuum-solidification combined method with sustainable alkali-activated binder. Geotext Geomembr 51(5):104–119. https://doi.org/10.1016/j.geotexmem. 2023.05.003
- Song DB, Pu HF, Lu MM, Zhang CX, Li ZY, Chen JNN (2023) Rapid treatment of mud slurry using a vacuum-assisted PHD and solidification combined method. Int J Geomech 23(9):04023134. https://doi.org/10.1061/IJGNAI.GMENG-8322
- Song DB, Pu HF, Yin ZY, Yin JH, Chen WB (2024) A novel analytical solution for slurry consolidation induced by a vacuumassisted prefabricated horizontal drain. J Geotech Geoenviron Eng 150(12):04024125. https://doi.org/10.1061/JGGEFK. GTENG-12044
- Sun Z, Chen WB, Zhao RD, Jin YF, Yin JH (2023) Solidification/ stabilization treatment of Hong Kong marine deposits slurry at high water content by ISSA and GGBS. Constr Build Mater 372:130817. https://doi.org/10.1016/j.conbuildmat.2023.130817
- Tang YX, Miyazaki Y, Tsuchida T (2001) Practices of reused dredgings by cement treatment. Soils Found 41(5):129–143. https://doi.org/10.3208/sandf.41.5\_129
- Terashi M (1980) Fundamental properties of lime and cement treated soils (2nd report). Rep Port Harbour Res Inst 19(1):33–57
- Watabe Y, Kaneko T, Watanabe Y (2016) Cement mix proportion for treated soils recycled from a cement treated soil. Jpn Geotech Soc Spec Publ 4:168–172. https://doi.org/10.3208/jgssp. v04.j16
- Watabe Y, Noguchi T (2011) Site-investigation and geotechnical design of D-runway construction in Tokyo Haneda Airport. Soils Found 51(6):1003–1018. https://doi.org/10.3208/sandf.51.1003
- Xiao P, Zhao G, Liu H (2022) Failure transition and validity of Brazilian disc test under different loading configurations: a numerical study. Mathematics 10(15):2681
- Xu F, Wei H, Qian W, Cai Y (2018) Composite alkaline activator on cemented soil: multiple-tests and mechanism analyses. Constr Build Mater 188:433–443. https://doi.org/10.1016/j.conbuildmat. 2018.08.118



- 62. Yin JH, Wong RHC, Chau KT, Lai DTW, Zhao GS (2017) Point load strength index of granitic irregular lumps: size correction and correlation with uniaxial compressive strength. Tunn Undergr Space Technol 70:388–399. https://doi.org/10.1016/j.tust.2017.09.011
- 63. Zhou YF, Lu JX, Li JS, Cheeseman C, Poon CS (2021) Hydration, mechanical properties and microstructure of lime-pozzolana

pastes by recycling waste sludge ash under marine environment. J Clean Prod 310:127441. https://doi.org/10.1016/j.jclepro.2021. 127441

**Publisher's Note** Springer Nature remains neutral with regard to jurisdictional claims in published maps and institutional affiliations.

